Organisms Diversity & Evolution
https://doi.org/10.1007/s13127-022-00550-2

ORIGINAL ARTICLE

Symbiodiniaceae diversity and characterization of palytoxin in various zoantharians (Anthozoa, Hexacorallia)

Ludovic Sawelew[1,2,3] · Christopher Nuccio[4] · Colin Foord[5] · Jean Lorquin[1] · Yvan Perez[2]

Received: 18 May 2021 / Accepted: 23 February 2022

Abstract

Anemone-like animals belonging to the order Zoantharia are common anthozoans widely distributed from shallow to deep tropical and subtropical waters. Some species are well-known because of their high toxicity due to the presence of palytoxin (PLTX) in their tissues. PLTX is a large polyhydroxylated compound and one of the most potent toxins known. Currently, the PLTX biosynthetic pathway in zoantharians and the role of the host or the putative symbiotic organism(s) involved in this pathway are entirely unknown. To better understand the presence of PLTX in some Zoantharia, twenty-nine zoantharian colonies were analysed in this study. All zoantharian samples and their endosymbiotic dinoflagellates (Symbiodiniaceae = Zooxanthellae) were identified using DNA barcoding and phylogenetic reconstructions. Quantification of PLTX and its analogues showed that the yields contained in *Palythoa heliodiscus*, *Palythoa* aff. *clavata* and one potentially undescribed species of *Palythoa* are among the highest ever found (up to > 2 mg/g of wet zoantharian). Mass spectrometry imaging was used for the first time on *Palythoa* samples and revealed that in situ distribution of PLTX is mainly located in ectodermal tissues such as the epidermis of the body wall and the pharynx. Moreover, high levels of PLTX have been detected in histological regions where few or no Symbiodiniaceae cells could be observed. Finally, issues such as host-specificity and environmental variables driving biogeographical patterns of hosted Symbiodiniaceae in zoantharian lineages were discussed in light of our phylogenetic results as well as the patterns of PLTX distribution. It was concluded that (1) the variability of Symbiodiniaceae diversity may be related to ecological divergence in Zoantharia, (2) all *Palythoa* species hosted *Cladocopium* Symbiodiniaceae (formerly clade C), (3) the sole presence of *Cladocopium* is not sufficient to explain the presence of high concentrations of PLTX and/or its analogues, and (4) the ability to produce high levels of PLTX and/or its analogues highlighted in some *Palythoa* species could be a plesiomorphic character inherited from their last common ancestor and subsequently lost in several lineages.

Keywords Liquid chromatography · Mass spectrometry imaging · *Palythoa* · Palytoxin · Phylogenetics · Symbiodiniaceae · *Zoanthus*

Jean Lorquin and Yvan Perez contributed equally to this work.

✉ Ludovic Sawelew
ludo.sawelew@gmail.com

[1] Mediterranean Institute of Oceanography (MIO) UM 110, Aix-Marseille University, CNRS, University of Toulon, Marseille, IRD, France

[2] Mediterranean Institute of Marine and Terrestrial Biodiversity and Ecology (IMBE) UMR 7263, Aix-Marseille University, University of Avignon, CNRS, Marseille, IRD, France

[3] Coral Biome SAS, Zone Luminy Entreprises, 163 avenue de Luminy, 13288 Marseille cedex 9, Marseille, France

[4] Membrane Transporters, Chemoresistance and Drug design UMR-MD1, Faculty Medical, Aix-Marseille University, Marseille, France

[5] Coral Morphologic Aquaculture Research Lab, 800 NW 7th Avenue Miami, Miami, FL 33136, USA

Introduction

Zoantharians (Anthozoa, Hexacorallia, Zoantharia) are sessile and usually colonial anemone-like animals widely distributed from shallow to deep tropical and subtropical waters. The order is mainly represented by the genera *Palythoa* Lamouroux, 1816 and *Zoanthus* Lamarck, 1801 that are morphologically similar. The molecular approach revealed that these two genera exhibit a wide intraspecific morphological plasticity, suggesting that previous systematics of *Palythoa* and *Zoanthus* species based on morphological characters (mainly the oral disk colour of polyps and several forms of colony growth) included a large number of synonyms (Burnett et al., 1997; Low et al., 2016; Reimer & Todd, 2009; Reimer et al., 2004, 2006a, 2012). Moreover, many of the remaining species exist in sibling pairs between the Atlantic and Indo-Pacific basins (Reimer et al., 2012). It is therefore almost impossible to tell species pairs apart without collection location and genetic data.

Although little is known about what exactly induces changes in the phenotype of zoantharians, some authors claimed that morphological variations in *Palythoa* and *Zoanthus* species may be a response to water turbidity (Costa et al., 2011), depth (Kamezaki et al., 2013) or, more generally, to light intensity (Ong et al., 2013). Morphological phenotypic plasticity would facilitate the colonization of a wide variety of habitats and help organisms adapt to changes in their environment (Burnett et al., 1997; Costa et al., 2011; Ong et al., 2013). Reimer et al. (2006b) observed that, due to volcanic ash incorporated into their tissues, samples of *Palythoa mutuki* (Haddon and Shackleton, 1891) and *Palythoa tuberculosa* (Esper, 1805) harvested in a volcanic area were darker in colour than samples harvested in non-volcanic areas. Moreover, Kamezaki et al. (2013) showed that specimens of *Zoanthus sansibaricus* Carlgren, 1900 sampled at different depth levels had different colours. Host-tissue colour variations of zoantharians could be due to the synthesis of different GFP-like proteins in response to different environmental parameters as observed in another Anthozoa, *Montastraea cavernosa* (Linnaeus, 1767) (Kelmanson & Matz, 2003). The use of phylogenetic analyses, particularly those based on a combination of mitochondrial and nuclear markers (Sinniger et al., 2008), is therefore more appropriate to identify zoantharian species and clarify the potentially numerous synonyms (Reimer et al., 2004, 2006a, 2012).

The genus *Palythoa* is known for comprising highly toxic species due to the presence of palytoxin (PLTX) in their tissues (Béress et al., 1983; Deeds et al., 2011; Moore & Scheuer, 1971). PLTX, one of the most toxic natural compounds ever discovered, is a non-protein marine toxin which consists of a long, partially unsaturated (with eight double bonds) aliphatic backbone with spaced cyclic ethers and 64 chiral centres (Uemura et al., 1985). Initially isolated from a *Palythoa* species (Moore & Scheuer, 1971), it can also be found in numerous other marine organisms from the same ecological region (Aratake et al., 2016). Moreover, several analogues of PLTX were discovered in various microorganisms (see Table 1). To date, *Palythoa heliodiscus* (Ryland & Lancaster, 2003) is the largest PLTX producer known among zoantharians with the highest recorded yield (1 mg of PLTX /g wet *Palythoa*) and deoxy-PLTX (3.51 mg/g wet *Palythoa* (Deeds et al., 2011)). However, in most cases the toxin yield in other *Palythoa* species is low. During the last decade, more attention was focused on PLTX because of (1) sanitary problems due to toxic *Ostreopsis* spp. outbreaks (Del Favero et al., 2012) or numerous cases of severe domestic poisoning from aquarium zoantharians (Barbany et al., 2019; Chang et al., 2020; Farooq et al., 2017; Gaudchau et al., 2019; Hall et al., 2015; Jalink & van Luijk, 2019; Moshirfar et al., 2010, 2021; Nordt et al., 2011; Ruiz et al., 2015; Schulz et al., 2019; Snoeks & Veenstra, 2012; Wonneberger et al., 2020), and (2) significant toxic effects on proliferation and survival of cancer cells (Kerbrat et al., 2011; Ledreux et al., 2009; Valverde et al., 2008). Consequently, there is a growing need for high-yield sources of PLTX to facilitate its functional characterization.

So far, the PLTX biosynthetic pathway and the respective roles of putative symbiotic organism(s) involved are entirely unknown (Aratake et al., 2016). The leading hypothesis, based on structural similarities observed between PLTX and zooxanthellatoxins (Drainville-Higgins, 2004; Nakamura et al., 1993; Onodera et al., 2004), proposed that endosymbiotic dinoflagellates (Symbiodiniaceae = zooxanthellae) are responsible for PLTX synthesis in *Palythoa*. Several species of free-living dinoflagellates are also able to produce PLTX and some analogues (Ciminiello et al., 2008; Lenoir et al., 2004; Rossi et al., 2010; Ukena et al., 2001). However, it is noteworthy that dinoflagellates are not the only organisms to produce PLTX or analogues. For example, PLTX and 42-hydroxy-PLTX are also produced by a marine Cyanobacteria belonging to the genus *Trichodesmium* (Kerbrat et al., 2011). Frolova et al. (2000) detected PLTX-like compounds in Gram-negative *Aeromonas* sp. and *Vibrio* sp. bacteria using anti-PLTX antibodies. Similarly, bacteria isolated from *Palythoa caribaeorum* (Duchassaing and Michelotti 1860) were found to display a PLTX-like haemolytic activity (Seemann et al., 2009) confirming that several prokaryotic organisms can produce at least one PLTX type. It is, therefore, possible to assume that the Symbiodiniaceae and symbiotic prokaryotes might collaborate to produce PLTX within their zoantharian host.

Table 1 Known molecules of the palytoxin family identified in Zoantharia, Cyanobacteria, algae, and dinoflagellates

Compound	Organism	MW	Concentration	Reference
Palytoxin	*Palythoa* sp.	2679	2220 µg/g wet	**This study (Z05)**
Palytoxin	*P.* aff. *clavata*	2679	1077 µg/g wet	**This study (Z26)**
Palytoxin	*P.* aff. *margaritae*	2679	ND	Oku et al. (2004)
Palytoxin	*P. canariensis*	2679	270 µg/g lyoph	Fraga et al. (2017)
Palytoxin	*P. caribaeorum*	2679	30 µg/g wet	Béress et al. (1983)
Palytoxin	*P. heliodiscus*	2679	minor	**This study (Z03, Z04)**
Palytoxin	*P. heliodiscus*	2679	515 µg/g wet	Deeds et al. (2011)
Palytoxin	*P. heliodiscus*	2679	613 µg/g wet	Deeds et al. (2011)
Palytoxin	*P. heliodiscus*	2679	1037 µg/g wet	Deeds et al. (2011)
Palytoxin	*P. heliodiscus*	2679	1164 µg/g wet	Deeds et al. (2011)
Palytoxin	*P. toxica*	2679	275 µg/g wet	Moore and Scheuer (1971)
Palytoxin	*P. tuberculosa*	2679	13.6 µg/g wet	Kimura and Hashimoto (1973)
Palytoxin[1]	*P. vestitus*	ND	ND	Quinn et al. (1974)
Palytoxin[2]	*Zoanthus sociatus*	ND	ND	Gleibs et al. (1995)
Palytoxin[2]	*Z. solanderi*	ND	ND	Gleibs et al. (1995)
Palytoxin-b	*P. tuberculosa*	2720	minor	Rossi et al. (2010)
Bishomo-palytoxin	*P. heliodiscus*	2706	1618 µg/g wet	**This study (Z07)**
Bishomo-palytoxin	*P. tuberculosa*	2706	minor	Uemura et al. (1985)
Deoxy-palytoxin[3]	*P. heliodiscus*	2663	3515 µg/g wet	Deeds et al. (2011)
Deoxy-palytoxin[3]	*P.* cf. *toxica*	2662	ND	Tartaglione et al. (2016)
Homo-palytoxin	*P. tuberculosa*	2692	minor	Uemura et al. (1985)
Neo-palytoxin	*P. tuberculosa*	2661	minor	Uemura et al. (1985)
OH-palytoxin[4]	*P.* cf. *toxica*	2695	ND	Tartaglione et al. (2016)
42-OH-palytoxin	*P. tuberculosa*	2695	minor	Ciminiello et al. (2009)
42-OH-palytoxin	*P. toxica*	2695	minor	Ciminiello et al. (2009)
42-OH-palytoxin[5]	*Trichodesmium* sp.	2695	minor	Kerbrat et al. (2011)
73-deoxy-palytoxin	*P. tuberculosa*	2663	minor	Uemura et al. (1985)
CA-I[6]	*Chondria armata*	ND	ND	Yasumoto and Murata (1990)
CA-II[6]	*C. armata*	ND	ND	Yasumoto and Murata (1990)
Mascarenotoxin-a	*Ostreopsis ovata*	2588	minor	Rossi et al. (2010)
Mascarenotoxin-a	*O. mascarenensis*	2588	minor	Lenoir et al. (2004)
Mascarenotoxin-b	*O. mascarenensis*	2606	minor	Lenoir et al. (2004)
Mascarenotoxin-c	*O. ovata*	2628	minor	Rossi et al. (2010)
Ostreocin-a	*O. siamensis*	2650	ND	Terajima et al. (2019)
Ostreocin-b	*O. siamensis*	2650	ND	Terajima et al. (2018)
Ostreocin-d	*O. siamensis*	2634	ND	Ukena et al. (2001)
Ostreocin-e1	*O. siamensis*	2616	ND	Terajima et al. (2019)
Ovatoxin-a	*O. ovata*	2646	minor	Ciminiello et al. (2008)
Ovatoxin-b	*O. ovata*	2662	minor	Rossi et al. (2010)
Ovatoxin-c	*O. ovata*	2690	minor	Rossi et al. (2010)
Ovatoxin-d	*O. ovata*	2706	minor	Rossi et al. (2010)

MW, molecular weight; *ND*, not determined. [1]In absence of mass spectrometry data, the toxin found in *Palythoa vestitus* displayed equivalent UV spectrum and toxicity against mice Ehrlich ascites tumour compared to *P. tuberculosa* toxin and is thought to synthesize a similar palytoxin (PLTX). [2]For *Zoanthus solanderi* Le Sueur, 1818 and *Zoanthus sociatus* (Ellis, 1768), presence of PLTX in the extracts was only shown by HPLC compared to the PLTX standard isolated from *P. caribaeorum* but has never been characterized by mass spectrometry. [3]Location of the deoxygenation was not determined for this analogue. [4]Position of the oxygenation was not determined for this analogue. [5]In this case, 42-hydroxy-PLTX was the main toxin and PLTX was present at only 10–20% of the total toxin amount. [6]CA-I and CA-II are two PLTX analogues in the red algae *Chondria armata* which mainly produces domoic acid

In an attempt to discover new valuable sources of PLTX and learn more about its biosynthetic pathway and storage into zoantharians, twenty-nine colonies were analysed. This study aims to compare the diversity of Symbiodiniaceae among closely related *Palythoa* and *Zoanthus* species and determine whether one or several Symbiodiniaceae could be related to high levels of PLTX in zoantharians. Our integrative results based on molecular analyses, HPLC, mass spectrometry, and MALDI-IMS strongly suggest that the "holobiont" (host plus its microbiote) plays a crucial role in the synthesis and storage of PLTX in Zoantharia, rather than Symbiodiniaceae alone.

Materials and methods

Biological material

Twenty-eight zoantharian colonies visually consistent with *Palythoa* or *Zoanthus* species and one colony morphologically similar (Z20) were used in the present study: eighteen specimens from Florida Miami ($n = 13$) and the Reunion Island ($n = 5$) have been collected by the teams of Coral Morphologic and Coral Biome respectively. The remaining ten colonies have been obtained from suppliers of the aquarium industry located in Indonesia (Table 2). Representative morphotypes of all samples are illustrated in supplementary information (Fig. A). Colonies were placed at Coral Biome's facility in the same recirculating aquaculture system connected to one biological filter fed by artificial seawater (Instant Ocean salts, from Seachem, Madison, USA). Parameters were as follows: temperature, 25–26 °C; density, 1023–1025 kg.m^{-3}; KH, 7–8°; pH, 8.2–8.4; Ca, 400–450 mg.l^{-1}; Mg, 1200–1300 mg.l^{-1}; nitrates < 5 mg.l^{-1}; phosphates < 0.1 mg.l^{-1}. Specimens were exposed to a daytime photoperiod of 12 h with an irradiance of 70 mol.quanta.m^{-2}.s^{-1} and fed twice a week with a powder of lyophilized copepods (*Calanus finmarchicus*) (Dupla, Gelsdorf, Germany) at a concentration of 700–900 µg/l.

DNA extraction, PCR amplification, and sequencing

To amplify both zoantharian and Symbiodiniaceae genes, tissue samples consisting of a complete oral disk (small polyps) or tentacles joined by a small piece of the oral disk (large polyps) were placed in 80% (v/v) alcohol. Total genomic DNA was extracted using the DNAeasy Kit (Qiagen, Valencia, CA).

Two commonly used DNA barcode markers (e.g. Reimer et al., 2012, 2013, 2014, 2017b) were amplified to identify the zoantharian species: the mitochondrial cytochrome oxidase subunit I (COI) and the entire length of the nuclear internal transcribed spacer region of ribosomal DNA (ITS-rDNA: internal transcribed spacer 1, 5.8S ribosomal RNA gene, internal transcribed spacer 2). COI sequences were amplified with the primers HCO2198 (5′—TAA ACT TCA GGG TGA CCA AAA AAT CA—3′) and LCO1490 (5′—GGT CAA CAA ATC ATA AAG ATA TTG G—3′). PCR amplifications were performed as follows: an initial denaturing step at 94 °C for 2 min followed by 5 cycles of 15 s denaturation at 92 °C, 45 s annealing at 48 °C followed by a gradual temperature increase up to 72 °C during 1 min, 1 min 30 extension at 72 °C, followed by 30 cycles of 15 s denaturation at 92 °C, 45 s annealing at 52 °C, 45 s extension at 72 °C, followed by 7 min at 72 °C. ITS-rDNA sequences were amplified using the primers Zoanf-ITS (5′—CTT GAT CAT TTA GAG GGA GT—3′) and Zoanr-ITS (5′—CGG AGA TTT CAA ATT TGA GCT—3′). The PCR program was carried out as follows: an initial denaturing step at 94 °C for 3 min, 35 cycles of 1 min denaturation at 94 °C, 1 min annealing at 50 °C, 2 min extension at 72 °C followed by 10 min at 72 °C.

To identify the Symbiodiniaceae genera associated with the zoantharian samples, the ITS2-rDNA sequences (5.8S ribosomal RNA, partial sequence; internal transcribed spacer 2, complete sequence; 28S ribosomal RNA gene, partial sequence) were amplified using the specific primers ITS2-F1 (5′—GAA TTG CAG AAC TCC GTG—3′) and ITS2-R2 (5′—ATA TGC TTA AAT TCA GCG GGT—3′). The ITS2-rDNA region remains the most used marker for analysing the diversity of Symbiodiniaceae (Shi et al., 2021).

PCR amplifications were performed under stringent conditions to specifically target the Symbiodiniaceae genes rather than those of zoantharians: an initial denaturing step at 94 °C for 3 min followed by 12 cycles of 45 s denaturation at 94 °C, 45 s annealing at 58 °C and an incremental decrease of 0.5 °C every cycle, 1 min extension at 72 °C, followed by 20 cycles of 45 s denaturation at 94 °C, 45 s annealing at 52 °C and 1 min extension at 72 °C followed by 7 min at 72 °C. After amplification, all PCR fragments were visualized by denaturing gradient gel electrophoresis and were directly sequenced (without a cloning step) in both directions using the amplicon primers with an ABI 96-capillary 3730XL sequencer at Eurofins Genomics (Ebersberg, Germany).

Phylogenetic analyses

Three data sets were used for molecular analyses: dataset 1 for zoantharian COI sequences, dataset 2 for zoantharian ITS-rDNA sequences and dataset 3 for Symbiodiniaceae ITS2-rDNA sequences. All sequences obtained in this study were first checked using NCBI BLAST, then aligned with orthologous sequences available in public databases using CLUSTALW implemented in BioEdit v7.1.9 (Hall, 1999). The program MUSCLE (Edgar, 2004) was used to carry out

Table 2 Sampling location of zoantharian colonies used in this study, sequences generated and species identification of Zoantharia and their endosymbiotic Symbiodiniaceae and palytoxin content

Sample ID	Sampling location	ITS-rDNA	COI	ITS2-rDNA	Identification from this study	Symbiodiniaceae hosted	Palytoxin content (mg/g wet)
Z01	Caribbean (Florida, Miami)	-	+	+	*Palythoa caribaeorum*	*Cladocopium*	Not detected
Z02	Caribbean (Florida, Miami)	+	+	+	*P. grandis*	*Cladocopium*	Not detected
Z03	Indo-Pacific	+	+	+	*P. heliodiscus*	*Cladocopium*	0.053 ± 0.003
Z04	Indo-Pacific	+	+	+	*P. heliodiscus*	*Cladocopium*	0.200 ± 0.034
Z05	Indo-Pacific	+	+	+	*P.* sp. Z05	*Cladocopium*	2.22 ± 0.041
Z06	Indo-Pacific	+	+	+	*P. mutuki*	*Cladocopium*	Not detected
Z07	Indo-Pacific	+	+	+	*P. heliodiscus*	*Cladocopium*	1.618 ± 0.434
Z08	Caribbean (Florida, Miami)	+	+	+	*Zoanthus solanderi*	*Symbiodinium*	/
Z09	Caribbean (Florida, Miami)	+	+	+	*Z. solanderi*	*Symbiodinium*	/
Z10	Caribbean (Florida, Miami)	+	+	+	*Z. solanderi*	*Symbiodinium*	/
Z11	Caribbean (Florida, Miami)	+	+	+	*Z. solanderi*	*Symbiodinium*	Not detected
Z12	Indo-Pacific	+	+	+	*Z. gigantus*	*Durusdinium*	/
Z13	Caribbean (Florida, Miami)	+	+	+	*Z. solanderi*	*Symbiodinium*	/
Z14	Indo-Pacific	+	+	+	*Z. kuroshio*	*Cladocopium*	/
Z15	Indo-Pacific	+	+	+	*Z. sansibaricus*	*Cladocopium*	/
Z16	Caribbean (Florida, Miami)	+	+	+	*Z. pulchellus*	*Cladocopium*	/
Z17	Indo-Pacific	+	+	+	*Z. sansibaricus*	*Cladocopium*	Not detected
Z18	Caribbean (Florida, Miami)	-	+	+	*Z. pulchellus*	*Symbiodinium*	/
Z19	Caribbean (Florida, Miami)	-	+	+	*Z. pulchellus*	*Symbiodinium*	/
Z20	Unknown	+	+	+	*Terrazoanthus* sp.	*Cladocopium*	Not detected
Z21	Indian Ocean (Reunion island)	+	+	+	*Z. kuroshio*	*Cladocopium*	/
Z22	Indian Ocean (Reunion island)	-	+	+	*Z. kuroshio*	*Cladocopium*	/
Z23	Indian Ocean (Reunion island)	+	+	+	*Z. sansibaricus*	*Symbiodinium*	/
Z24	Indian Ocean (Reunion island)	+	+	+	*Z. sansibaricus*	*Cladocopium*	/
Z25	Indian Ocean (Reunion island)	+	+	+	*Z. sansibaricus*	*Cladocopium*	/
Z26	Caribbean (Florida, Miami)	+	+	+	*P.* aff. *clavata*	*Cladocopium*	1.077 ± 0.072
Z27	Caribbean (Florida, Miami)	+	+	+	*P.* aff. *clavata*	*Cladocopium*	1.265 ± 0.181
Z28	Caribbean (Florida, Miami)	+	+	+	*Z. sociatus*	*Symbiodinium*	/
Z29	Indo-Pacific	+	+	+	*P. mutuki*	*Cladocopium*	Not detected

COI, mitochondrial cytochrome oxidase subunit I; *ITS2-rDNA*, internal transcribed spacer 2 of ribosomal DNA; *ITS-rDNA*, complete nuclear internal transcribed spacer region of ribosomal DNA; /, not investigated in this study; +, sequence generated; -, not acquired

a multiple alignment of ITS2-rDNA sequences (dataset 3). For each dataset, the program MODELTEST v3.0b4 (Posada & Crandall, 1998) was used to determine the best model of DNA evolution using the Bayesian information criterion (BIC). Molecular analyses were conducted through neighbour-joining (NJ) and maximum likelihood (ML) methods using MEGA v7.0 (Tamura et al., 2013). Bayesian inference (BI) was performed with MrBayes v3.2 (Ronquist & Huelsenbeck, 2003). Topological robustness was determined using 100 non-parametric bootstrap replicates for NJ and ML analyses. For BI, Markov Chain Monte Carlo searches were done with four chains for 1,000,000 generations, with a random starting tree, default priors and Markov chains (with default heating values) sampled every 1,000 generations. It must be noted that previous studies have shown that *Zoanthus sansibaricus* collected along the Japanese coasts (Aguilar & Reimer, 2010; Reimer et al., 2007) and in the Red Sea (Reimer et al., 2017a) possesses two distinct types of ITS-rDNA sequences: a "normal" type that is closely related to *Zoanthus gigantus* ITS-rDNA sequences and a "distant" type, which is more divergent. According to the specimen considered, three combinations of alleles were identified:

"normal" only, "distant" only, or both (Aguilar & Reimer, 2010; Reimer et al., 2007).

MALDI-IMS analyses and localization of Symbiodiniaceae cells in *Palythoa*

Polyps were collected from cultured colonies, harvested with care and then quickly frozen in a container of isopentane plunged in liquid nitrogen. After 5 min, dry polyps were stored at − 80 °C overnight. Tissue sections were cut using a Leica CM 1900 UV Microsystems cryostat (Leica Microsystems SAS) with a microtome chamber and a specimen holder chilled at − 20 °C. Sections of 18 µm were cut in crosswise directions at three levels of the polyp body. Lengthwise sections were also made in some specimens. Sections were thaw mounted onto Indium Tin Oxide coated microscopic slides (Bruker Daltonics) adapted for MALDI-IMS, and onto Superfrost plus slides (Thermo Scientific) for epifluorescence imaging. Both types of target slides were dried in a desiccator for 45 min. Polyp sections were scanned before matrix deposition with a histology slide scanner (Opticlab H850 scanner, Plustek). Then, 2,5-dihydroxybenzoic (DHB) acid (Bruker, Daltonics) 30 mg/ml in 50/50 (v/v) MeOH/H_2O containing 0.1% (v/v) trifluoroacetic acid (TFA) was used as a matrix and applied on sections using an automatic matrix sprayer (TM-Sprayer, HTX Technologies). MALDI calibration was carried out manually with Peptide Calibration Standard 2 (Bruker Daltonics). MALDI-IMS data acquisition was performed on an Ultraflextreme mass spectrometer using the FlexControl 3.3 software (Bruker Daltonics) in positive reflectron mode and FlexImaging 3.0. The measurement regions were manually defined and surimposed with the histological images. The spatial resolution was set at 30 µm with a laser diameter of 20 µm, and 300 laser shots were accumulated for each spot. The laser power was optimized at the start directly on tissue and then fixed for the overall MALDI-IMS experiment. The images were opened with SCILS Lab v2.5 in RAW data with a baseline subtraction to maintain the resolution of the average mass spectrum. Due to the high intensity of the PLTX signal, root mean square normalization was chosen for better visualization of the distribution. Endogenous autofluorescence of chlorophyll and peridinin pigments of the Symbiodiniaceae cell was revealed under an inverted microscope (Nikon Eclipse TE2000-U) using a filter cube B-2E/C corresponding to a medium band blue excitation. Images were acquired with the NIS-Elements BR v2.30 imaging software.

PLTX extraction and purification

About one gram of entire zoantharian polyps was gently detached from the colony with a scalpel, chopped into several pieces and placed in 20 ml of 80% (v/v) MeOH in milliQ H_2O. MeOH was evaporated using a rotavapor and the aqueous phase extracted several times with dichloromethane to remove carotenoid and chlorophyll pigments. The aqueous phase containing PLTX was evaporated and deposited onto a 2 cm diameter glass column filled with 10 cm^3 of C_{18} reversed-phase powder (Lichroprep RP_{18}, from MERCK, France). The column was washed with acidified H_2O (0.2% (v/v) formic acid), then with 50% (v/v) MeOH in acidified H_2O. PLTX was finally eluted with 75% (v/v) MeOH in acidified H_2O, and a dried pale-yellow solid of purified PLTX was obtained after N_2 flow evaporation. The toxin was solubilised in dimethyl sulfoxide (DMSO) and quantified using high-performance liquid chromatography (HPLC, see below). PLTX was then stored at concentrations comprised between 25 and 100 µg/µl at 4 °C in darkness.

Fig. 1 Mid-rooted maximum-likelihood phylogenetic tree based on zoantharian mitochondrial cytochrome oxidase subunit I (COI) sequences. Support values obtained using different reconstruction methods are indicated at branch nodes (maximum likelihood, *ML*; neighbour joining, *NJ*; and Bayesian inference, *BI*). Support values are displayed when $ML > 80$, $NJ > 85$, or $BI > 0.85$. Sequences newly obtained in this study are represented in bold. Sequences from previous studies are included with GenBank accession numbers and location when available

HPLC analyses and PLTX quantifications

Solvents were of HPLC grade from Biosolve (Dieuze, France). To control the purity of the PLTX fraction and quantify the toxin, 2–5 µg of PLTX in DMSO were injected and analysed by reverse-phase (RP) HPLC with a Waters equipment composed of a 1525 binary pump, a 2996 diode array detector, a 7725i Rheodyne injector fitted with a 20 µl loop, and a temperature control system. Files were acquired with the Empower software. Separations were carried out on a Cortecs RP-C_{18} column (4.6 × 75 mm, 2.7 µm) protected with a guard cartridge. Elution was performed at 30 °C, at a flow rate of 0.8 ml/min with two linear gradients using solvent A (acetonitrile containing 0.2% (v/v) acetic acid) and solvent B (H_2O containing 0.2% (v/v) acetic acid): 5 to 100% A for 10 min then 100 to 5% A for 2 min. PLTX was visualized at 263 nm and total spectra were analysed from 200 to 700 nm with the Empower software. PLTX peak areas were measured and interpolated within a calibration curve established with commercial PLTX (from Wako Pure Chemical Industries, Japan) dissolved in DMSO. The linearity of the calibration curve was indicated by a correlation coefficient (R^2) of 0.9948. PLTX concentration in each zoantharian sample was determined by averaging the results obtained from 3 extractions. When PLTX was not detected by HPLC in purified coral extracts, the calculated detection limit was 9 ng/mL at λ 265 nm and 5 ng/mL at λ 235 nm, the absence of the characteristic ions (bis-charged and molecular ions)

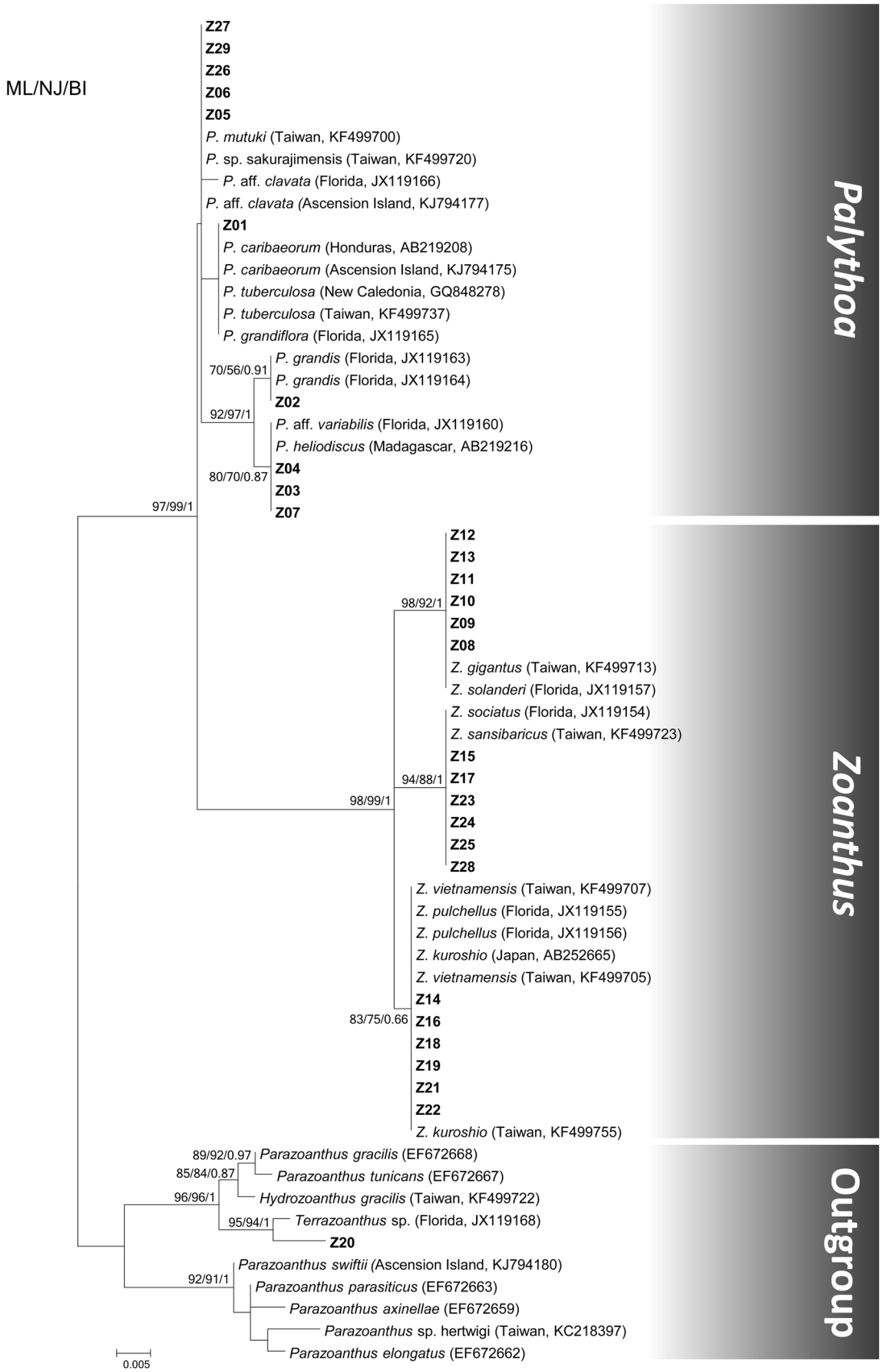
ML/NJ/BI
Z27
Z29
Z26
Z06
Z05
P. mutuki (Taiwan, KF499700)
P. sp. sakurajimensis (Taiwan, KF499720)
P. aff. clavata (Florida, JX119166)
P. aff. clavata (Ascension Island, KJ794177)
Z01
P. caribaeorum (Honduras, AB219208)
P. caribaeorum (Ascension Island, KJ794175)
P. tuberculosa (New Caledonia, GQ848278)
P. tuberculosa (Taiwan, KF499737)
P. grandiflora (Florida, JX119165)
70/56/0.91
P. grandis (Florida, JX119163)
P. grandis (Florida, JX119164)
Z02
92/97/1
P. aff. variabilis (Florida, JX119160)
P. heliodiscus (Madagascar, AB219216)
80/70/0.87
Z04
Z03
Z07
97/99/1
Z12
Z13
Z11
98/92/1
Z10
Z09
Z08
Z. gigantus (Taiwan, KF499713)
Z. solanderi (Florida, JX119157)
Z. sociatus (Florida, JX119154)
Z. sansibaricus (Taiwan, KF499723)
Z15
94/88/1
Z17
98/99/1
Z23
Z24
Z25
Z28
Z. vietnamensis (Taiwan, KF499707)
Z. pulchellus (Florida, JX119155)
Z. pulchellus (Florida, JX119156)
Z. kuroshio (Japan, AB252665)
Z. vietnamensis (Taiwan, KF499705)
Z14
83/75/0.66
Z16
Z18
Z19
Z21
Z22
Z. kuroshio (Taiwan, KF499755)
89/92/0.97
Parazoanthus gracilis (EF672668)
85/84/0.87
Parazoanthus tunicans (EF672667)
96/96/1
Hydrozoanthus gracilis (Taiwan, KF499722)
95/94/1
Terrazoanthus sp. (Florida, JX119168)
Z20
Parazoanthus swiftii (Ascension Island, KJ794180)
92/91/1
Parazoanthus parasiticus (EF672663)
Parazoanthus axinellae (EF672659)
Parazoanthus sp. hertwigi (Taiwan, KC218397)
Parazoanthus elongatus (EF672662)
0.005
Palythoa
Zoanthus
Outgroup

in mass spectrometry (LC-QToF) systematically confirmed the absence of the toxin in these corals.

Mass spectrometry

Identification of mass spectra was done on an accurate mass spectrometer Agilent 6530 Q-TOF–MS (Agilent Technologies, USA). Chromatographic separation was performed on an RP-C_{18} Cortecs column (4.6 × 75 mm, 2.7 µm, Waters, UK) protected with a guard cartridge. The effluent of the HPLC mobile phase was split and guided into the electrospray ionization (ESI) source. Parameter conditions were performed as follows: capillary voltage, 3000 V; nebulizer pressure, 45 psi; nozzle voltage, 500 V; flow rate of drying gas, 7 l/min; temperature of sheath gas, 300 °C; flow rate of sheath gas, 10 l/min; skimmer voltage, 65 V; OCT1 RF Vpp, 750 V; fragmentor voltage, 175 V. Elution was performed at 30 °C at a flow rate of 0.4 ml/min with three linear gradients using solvent A (acetonitrile containing 0.2% (v/v) acetic acid) and solvent B (H_2O containing 0.2% (v/v) acetic acid): 20 to 60% A for 35 min, 60 to 100% A for 5 min, and 100 to 20% A for 5 min. The calibration was performed with a solution of CsI 1 mg/ml and used in the 100 – 3200 mass range with a precision of +/− 3 ppm. The data of the selected compounds were obtained by regulating diverse collision energy between 45 and 100 eV.

Results

Molecular phylogenetic analyses

Whatever the dataset considered, the BI and NJ trees presented similar topologies to the ML bootstrapped trees. Thus, their statistical values were reported onto the ML topology. Analyses were carried out with sequences from Parazoanthidae and Hydrozoanthidae used as outgroups.

COI and ITS-rDNA sequences of zoantharians

Both COI and ITS-rDNA markers were generated for 25 of 29 specimens (Table 2). For the remaining four specimens, only COI sequences were successfully generated. All failed sequences were attempted at least three times. The resulting alignment of COI sequences had a length of 402 bp (dataset 1), while ITS-rDNA had aligned lengths of 760 bp (dataset 2). All sequences have been deposited in GenBank with accession numbers MW717422 to MW717450 for COI and MW219226 to MW219250 for ITS-rDNA. Distances were calculated using a Kimura's 2-parameter model (Kimura, 1980) with either a discrete gamma distribution (K2 + Γ, lnL = − 957.423, dataset 1) or a proportion of invariable sites (K2 + I, lnL = − 1234.887, dataset 2). BI

Fig. 2 Mid-rooted maximum-likelihood phylogenetic tree based on zoantharian internal transcribed spacer of ribosomal DNA (ITS-rDNA) sequences. Support values obtained using different reconstruction approaches are indicated at branch nodes (maximum likelihood, *ML*; neighbour joining, *NJ*; and Bayesian inference, *BI*). Support values are displayed when *ML* > 80, *NJ* > 85, or *BI* > 0.85. Sequences newly obtained in this study are represented in bold. Sequences from previous studies are included with GenBank accession numbers and location when available

were performed using an HKY model (Hasegawa et al., 1985) with stationary state frequencies fixed to equal to get a Kimura's 2-parameter model (prset statefreqpr = fixed (equal)) either with a gamma-distributed rate (dataset 1) or a proportion of invariant sites (dataset 2).

The mid-rooted phylogenetic trees based on zoantharian COI sequences had very similar topologies whatever the method considered (Fig. 1). Sequences from all *Palythoa* plus *Zoanthus* species (suborder Brachycnemina) constituted a strongly supported monophyletic group (97/99/1, NJ/ML/BI). Within this clade, the *Zoanthus* monophyly (Zoanthidae) was similarly strongly supported (98/99/1) while the *Palythoa* monophyly (Sphenopidae) was moderately supported (71/65/0.71). Among the *Palythoa* species, sequences from specimens Z05, Z06, Z26, Z27, and Z29 were identical to *P. mutuki* (KF499742, Taiwan), *P.* aff. *clavata* (KJ794177, Ascension Island), and *P.* sp. "sakurajimensis" (KF499720, Taiwan). These sequences constituted a basal polytomy that included a sequence of *P.* aff. *clavata* (JX119166, Florida) which differed only by a single base (C → T, position 377). Sequences from specimen Z01, *P. caribaeorum* (AB219208, Honduras; KJ794175, Ascension Island), *P. tuberculosa* (GQ848278, New Caledonia; KF499737, Taiwan), and *P. grandiflora* Verrill, 1900 (JX119165, Florida) were also identical. The other *Palythoa* sequences constituted a well-supported monophyly (92/97/1) containing two sister clades. The first was moderately supported (70/56/0.91) and comprised two sequences of *Palythoa grandis* Verrill, 1900 along with the sequence amplified from specimen Z02. The second well-supported clade (80/70/0.87) represented the Caribbean/Indo-Pacific sister species complex of *Palythoa variabilis* (Duerden, 1898)*/heliodiscus*. In this assemblage, sequences from specimens Z03, Z04, and Z07 were identical to *P.* aff. *variabilis* (JX119160, Florida) and *P. heliodiscus* (AB219216, Madagascar). In Zoanthidae, three main lineages were successfully recovered as monophyletic groups. The first one (98/92/1) constituted the Caribbean/Indo-Pacific sister species complex of *Z. solanderi/gigantus* and included identical sequences from specimens Z08–Z13, *Z. gigantus* (KF499713, Taiwan) and *Z. solanderi* (JX119157, Florida). The second well-supported lineage (94/88/1) represented the sister species complex of *Z. sociatus/sansibaricus* including the sequence from specimen Z28 and identical sequences

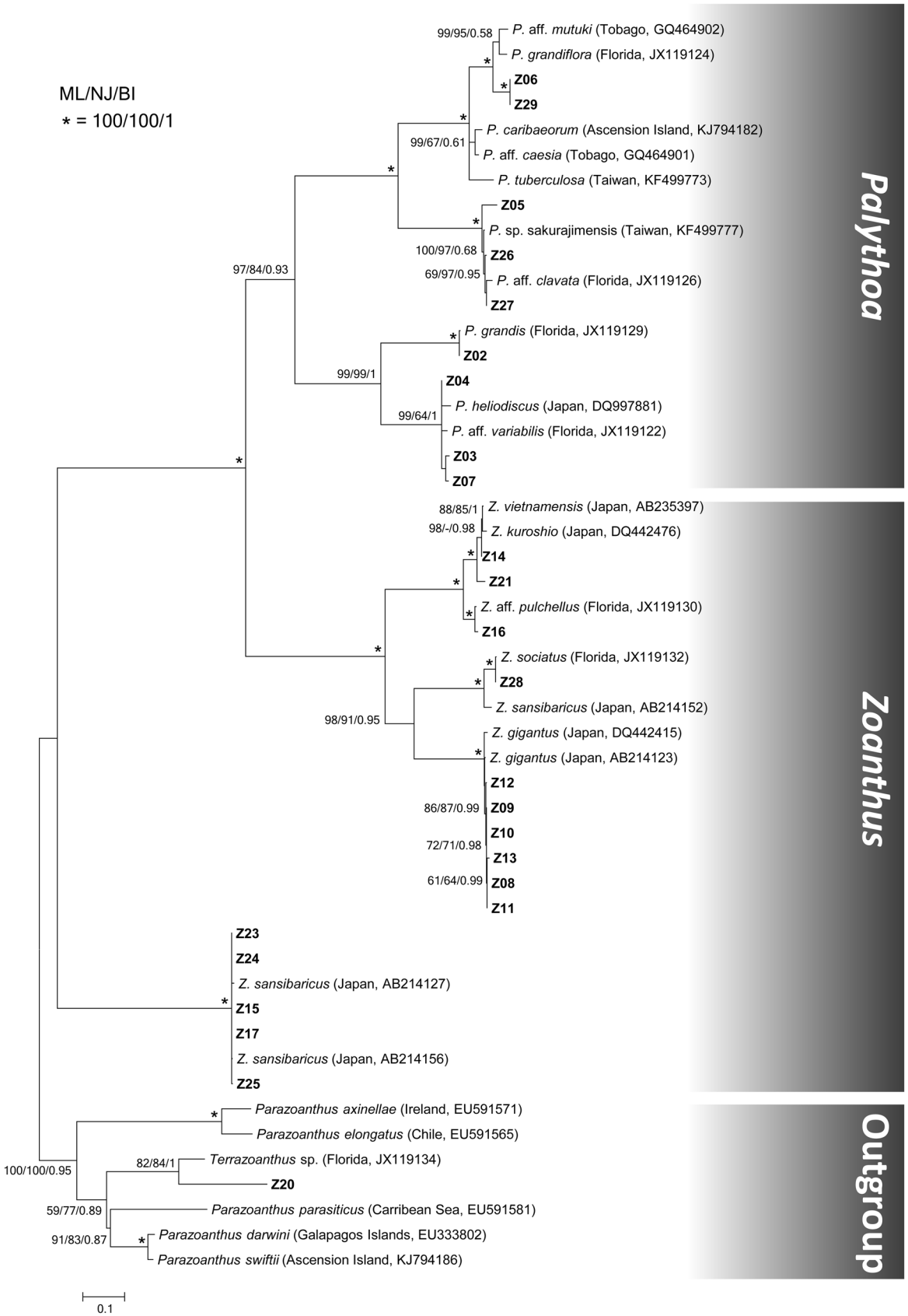
ML/NJ/BI
* = 100/100/1
99/95/0.58
P. aff. mutuki (Tobago, GQ464902)
P. grandiflora (Florida, JX119124)
Z06
Z29
P. caribaeorum (Ascension Island, KJ794182)
99/67/0.61
P. aff. caesia (Tobago, GQ464901)
P. tuberculosa (Taiwan, KF499773)
Z05
P. sp. sakurajimensis (Taiwan, KF499777)
100/97/0.68
Z26
97/84/0.93
69/97/0.95
P. aff. clavata (Florida, JX119126)
Z27
P. grandis (Florida, JX119129)
Z02
99/99/1
Z04
P. heliodiscus (Japan, DQ997881)
99/64/1
P. aff. variabilis (Florida, JX119122)
Z03
Z07
Palythoa
88/85/1
Z. vietnamensis (Japan, AB235397)
98/-/0.98
Z. kuroshio (Japan, DQ442476)
Z14
Z21
Z. aff. pulchellus (Florida, JX119130)
Z16
Z. sociatus (Florida, JX119132)
Z28
Z. sansibaricus (Japan, AB214152)
98/91/0.95
Z. gigantus (Japan, DQ442415)
Z. gigantus (Japan, AB214123)
Z12
86/87/0.99
Z09
Z10
72/71/0.98
Z13
61/64/0.99
Z08
Z11
Zoanthus
Z23
Z24
Z. sansibaricus (Japan, AB214127)
Z15
Z17
Z. sansibaricus (Japan, AB214156)
Z25
Parazoanthus axinellae (Ireland, EU591571)
Parazoanthus elongatus (Chile, EU591565)
82/84/1
Terrazoanthus sp. (Florida, JX119134)
100/100/0.95
Z20
59/77/0.89
Parazoanthus parasiticus (Carribean Sea, EU591581)
91/83/0.87
Parazoanthus darwini (Galapagos Islands, EU333802)
Parazoanthus swiftii (Ascension Island, KJ794186)
Outgroup
0.1

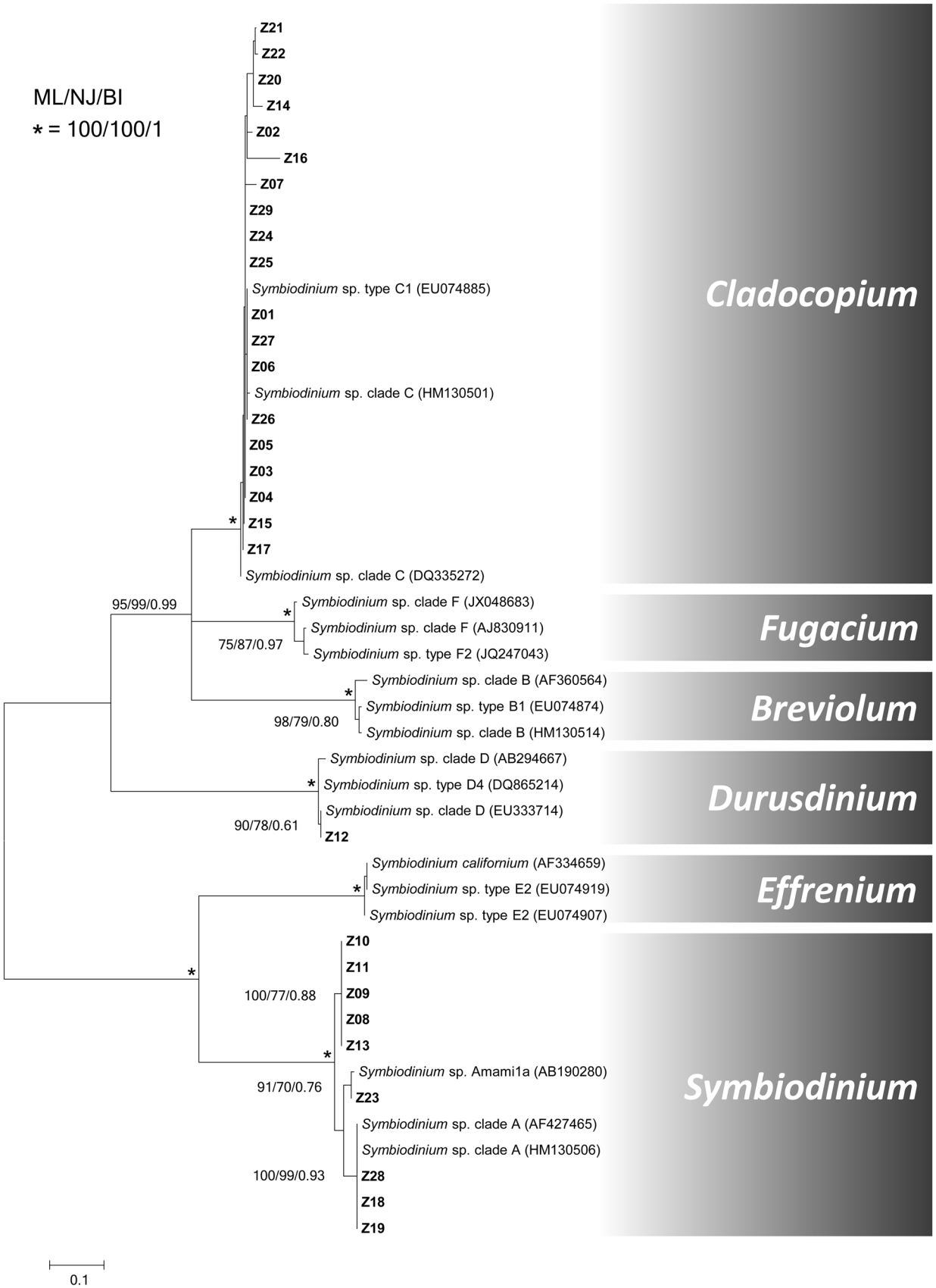
ML/NJ/BI
* = 100/100/1
Z21
Z22
Z20
Z14
Z02
Z16
Z07
Z29
Z24
Z25
Symbiodinium sp. type C1 (EU074885)
Z01
Z27
Z06
Symbiodinium sp. clade C (HM130501)
Z26
Z05
Z03
Z04
Z15
Z17
Symbiodinium sp. clade C (DQ335272)
95/99/0.99
Symbiodinium sp. clade F (JX048683)
Symbiodinium sp. clade F (AJ830911)
75/87/0.97
Symbiodinium sp. type F2 (JQ247043)
Symbiodinium sp. clade B (AF360564)
Symbiodinium sp. type B1 (EU074874)
98/79/0.80
Symbiodinium sp. clade B (HM130514)
Symbiodinium sp. clade D (AB294667)
Symbiodinium sp. type D4 (DQ865214)
Symbiodinium sp. clade D (EU333714)
90/78/0.61
Z12
Symbiodinium californium (AF334659)
Symbiodinium sp. type E2 (EU074919)
Symbiodinium sp. type E2 (EU074907)
Z10
Z11
100/77/0.88
Z09
Z08
Z13
Symbiodinium sp. Amami1a (AB190280)
91/70/0.76
Z23
Symbiodinium sp. clade A (AF427465)
Symbiodinium sp. clade A (HM130506)
100/99/0.93
Z28
Z18
Z19
0.1
Cladocopium
Fugacium
Breviolum
Durusdinium
Effrenium
Symbiodinium

◂**Fig. 3** Maximum-likelihood tree of Symbiodiniaceae internal transcribed spacer of ribosomal DNA (ITS-2) sequences. Support values obtained using different reconstruction approaches are indicated at branch nodes (maximum likelihood, *ML*; neighbour joining, *NJ*; and Bayesian inference, *BI*). Support values are displayed when $ML > 80$, $NJ > 85$, or $BI > 0.85$. Sequences newly obtained in this study are represented in bold. Sequences from previous studies are included with GenBank accession numbers and location when available

from specimens Z15, Z17, Z23–Z25, *Z. sansibaricus* (KF499723, Taiwan) and *Z. sociatus* (JX119154, Florida). Finally, the sequences from specimens Z14, Z16, Z18, Z19, Z21, and Z22 were identical to *Zoanthus vietnamensis* (Pax & Mueller, 1957) (KF499705, Taiwan), *Zoanthus pulchellus* (Duchassaing and Michelotti, 1860) (JX119156, Florida), and *Zoanthus kuroshio* (Reimer et al., 2007) (AB252665, Japan). These last sequences formed a third monophyletic lineage (83/75/0.66) corresponding to the sibling species pair *Z. pulchellus/kuroshio*.

The monophyly of the genus *Palythoa* (Sphenopidae) was strongly confirmed (97/84/0.93) in phylogenetic reconstructions based on ITS-rDNA sequences (Fig. 2). Whatever the method considered, the sibling species pairs of *Palythoa* from Caribbean or Indo-Pacific basins were fully recovered with high support values: (1) *P. caribaeorum/tuberculosa* (100/100/1) along with a first subclade composed of the sequences from Z06 and Z29 specimens (100/100/1) the latter being sister group to a second sublade composed of *P.* aff. *mutuki* and *P. grandiflora* (99/96/0.58), (2) *P.* aff. *clavata*/sp. "sakurajimensis" (100/100/1) including the sequences from Z05, Z26, and Z27 specimens, (3) a clade strongly supported (99/99/1) composed of two sister groups: *P. variabilis/heliodiscus* and the sequences from Z03, Z04, and Z07 on the one hand (99/64/1), and *P. grandis* plus Z02 on the other (100/100/1). Moreover, the ITS-rDNA analyses confirmed the sister group relationships of Z20 and *Terrazoanthus* sp. (82/84/1). While the validity of the Caribbean/Indo-Pacific sibling species pairs *Z. pulchellus/kuroshio* (100/100/1), *Z. sociatus/sansibaricus* (100/100/1), and *Z. solanderi/gigantus* (100/100/1) was confirmed, the Zoanthidae appeared paraphyletic in the ITS-rDNA trees because of the presence of an additional allele (the "distant" allele) previously amplified in *Z. sansibaricus* and several related specimens (Z15, Z17, Z23 – Z25). No "normal" allele could be identified in the *Z. sansibaricus* specimens analysed in this study, a result which confirms that the "distant" allele is much more common (for an explanation on the origin of the "distant" and "normal" ITS-rDNA alleles see Aguilar & Reimer, 2010).

ITS2-rDNA sequences of Symbiodiniaceae

In this study, we used the taxonomic nomenclature given by LaJeunesse et al. (2018) who revised the Symbiodiniaceae systematics and divided the former genus *Symbiodinium* into seven new genera: *Symbiodinium*, *Breviolum*, *Cladocopium*, *Durusdinium*, *Effrenium*, *Fugacium*, and *Gerakladium* (formerly described as clades A, B, C, D, E, F, and G, respectively). Symbiodiniaceae ITS2-rDNA sequences were successfully generated from all zoantharian specimens (Table 2). After the sequencing step, the ITS2-rDNA sequence displayed clear chromatograms in both forward and reverse directions with no "double-peaks" or mixed signals. Therefore, there was no need for a cloning step to investigate the intragenomic variability. Although several Symbiodiniaceae taxa may be hosted by a single zoantharian colony, a unique one is commonly found to be predominant. When distinct Symbiodiniaceae are hosted by the same coral, they usually belong to distinct genera (see Hume et al., 2019 and references therein). Therefore, the sequences obtained in this study were interpreted as representing the sole or dominant Symbiodiniaceae genus in each sample.

The sequences isolated from all the 29 samples (Table 2), together with GenBank sequences, built up a total dataset of 47 sequences. The new Symbiodiniaceae sequences have been deposited in GenBank with accession numbers MW077616 to MW077644. The complete alignment displayed 277 positions (dataset 3). Distances were calculated using a Kimura's 2-parameter model (Kimura, 1980) with a proportion of invariable sites ($K2 + I$ $\ln L = -1956.876$). Phylogenetic analyses of ITS2-rDNA sequences, which were rooted on the midpoint, yielded well-resolved trees in which the main genera of Symbiodiniaceae previously described in cnidarians received high support values whatever the method considered (Fig. 3). Symbiodiniaceae belonging to the genus *Cladocopium* (formerly the generalist clade C) were identified in all *Palythoa* (Z01–Z07, Z26, and Z27) as well as in the *Terrazoanthus* (Z20) and nine *Zoanthus* specimens (Z14–Z17, Z21, Z22, Z24, Z25, and Z29). The sequence amplified from specimen Z12 constituted a well-supported group with the sequence EU333714 (90/78/0.61) within the genus *Durusdinium* (formerly clade D). ITS2-rDNA sequences belonging to the genus *Symbiodinium* (formerly clade A) were divided into three well-supported subclades: the sequences Z08–Z11 and Z13 (100/77/0.88); the sequences Z18, Z19, Z28 along with the GenBank sequences AF427465 and HM130506 (100/99/0.93); the sequences Z23 and AB190280 (91/70/0.76).

Purification, quantification, and characterization of PLTX

All samples identified as *Palythoa* (Z01–Z07, Z26, Z27, and Z29), *Terrazoanthus* species (Z20) and two *Zoanthus* samples containing either *Symbiodinium* (Z11) or *Cladocopium* (Z17), were extracted and the presence of PLTX was analysed using high-performance liquid chromatography

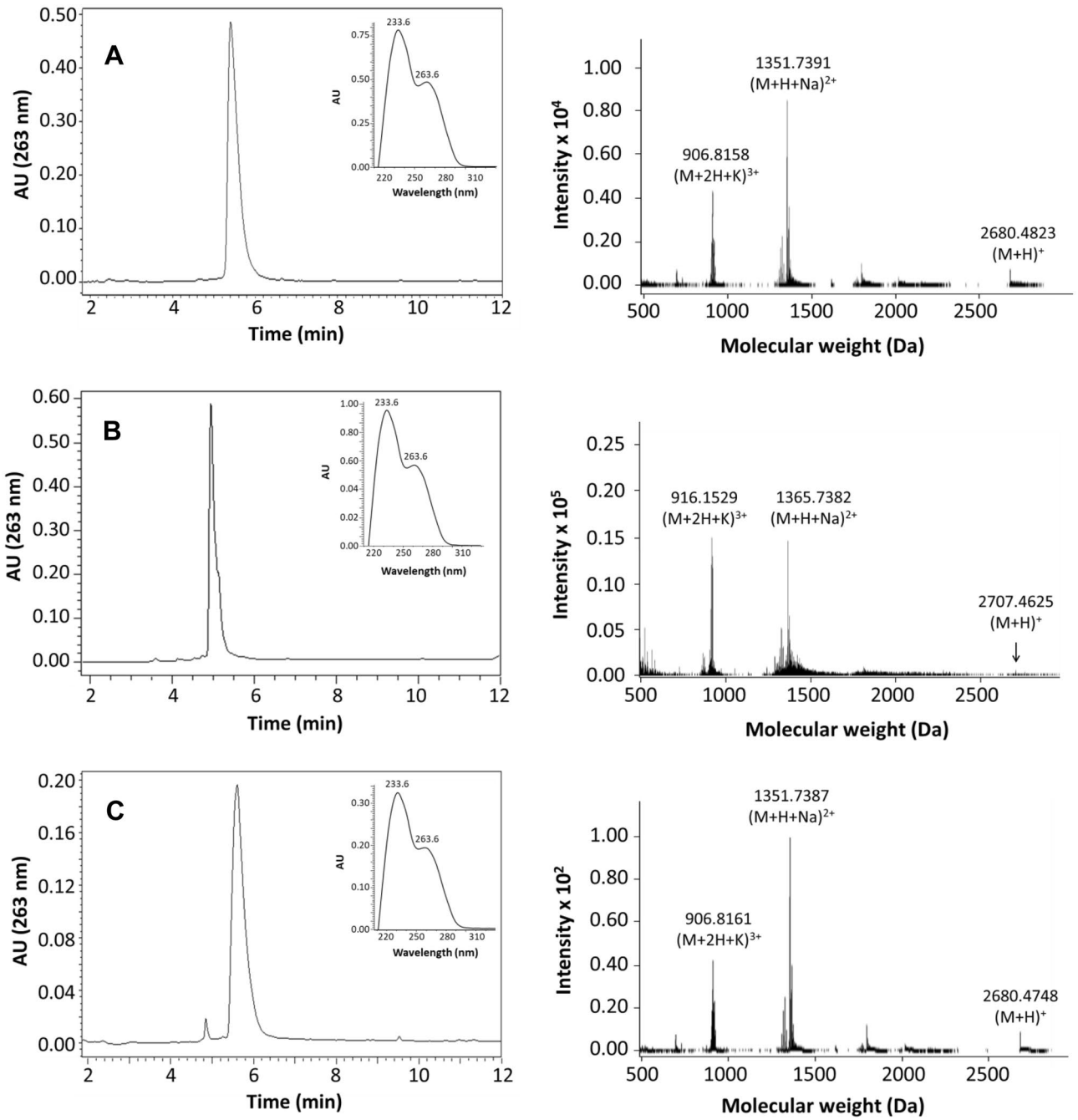

Fig. 4 High-performance liquid chromatography profile at 263 nm (left column) and high-resolution mass spectrometric analysis (right column) of PLTX extracted from **A** *Palythoa* sp. Z05, **B** *Palythoa heliodiscus* (Z07), and **C** *Palythoa* aff. *clavata* (Z26). The inserted graph in the left column shows the UV spectra of the toxin at the HPLC 263 nm peak apex. All samples contained a 327 Da fragment and UV maxima at 233 and 263 nm, which are characteristic of PLTX and the majority of its analogues

(HPLC–DAD). Measurement of PLTX concentration by HPLC–DAD has some limitations as the method does not allow for identification of PLTX analogues eluting at the same time. PLTX concentrations measured by HPLC should be considered the total concentrations of PLTX and/or its analogues. In each positive sample, PLTX peaks (retention time around 5.2 to 5.6 min) displayed two characteristic UV bands at 233 and 263 nm. For each specimen, PLTX concentrations were quantified in triplicate within a calibration curve established with PLTX standard (Wako Pure Chemical Industries, Japan). The purity was first controlled by HPLC–DAD in the entire UV–visible range showing the absence of analogue or other absorbing impurities (200–600 nm), and further confirmed by LC-QToF mass

spectrometry (see below). The concentrations of PLTX in samples, expressed in milligrams of toxin per gram of wet zoantharian, were determined by averaging 3 extractions. PLTX was detected in 6 *Palythoa* samples (Z03, Z04, Z05, Z07, Z26, Z27, Table 2). No PLTX was detected in *P. caribaeorum* (Z01), *P. grandis* (Z02), *P. mutuki* (Z06 and Z29), *Terrazoanthus* sp. (Z20), and *Zoanthus* samples (Z11 and Z17) despite at least two attempts with final DMSO solutions highly concentrated to increase the HPLC detection threshold. The highest PLTX concentrations were measured in *Palythoa* sp. Z05 (2.22 ± 0.041 mg/g wet), *P. heliodiscus* (Z07, 1.618 ± 0.434 mg/g wet), and *P.* aff. *clavata* (Z26, 1.077 ± 0.072 mg/g wet; Z27, 1.265 ± 0.181 mg/g wet). Lower PLTX concentrations were detected in two others *P. heliodiscus* samples (Z03, 0.053 ± 0.003 mg/g wet; Z04, 0.200 ± 0.034 mg/g wet). Three highly toxic samples were analysed using mass spectrometry (Fig. 4). The toxin extracted from *Palythoa* sp. Z05 and *P.* aff. *clavata* (Z26) displayed a clear ion profile corresponding to PLTX with prominent tri-charged $[M+2H+K]^{3+}$ (*m/z* 906.8158 and 906.8161, respectively), bi-charged $[M+H+Na]^{2+}$ (*m/z* 1351.7391 and 1351.7387, respectively), and mono-charged $[M+H]^{+}$ (*m/z* 2680.4823 and 2680.4748, respectively) molecular ions corresponding to a molecular mass of 2679 Da. The chromatogram of Z26 showed a small peak eluting before PLTX. Its composition was not determined, and it could correspond to impurities that were not removed during extraction or to PLTX degradation products. The toxin fraction extracted from *P. heliodiscus* (Z07) displayed prominent ions at *m/z* 916.1529 $[M+2H+K]^{3+}$, 1365.7382 $[M+H+Na]^{2+}$ and 2707.4625 $[M+H]^{+}$ corresponding to a molecular mass of 2706 Da. This ion profile is typical to the bishomo-PLTX. Moreover, besides these ions, small peaks were also seen at *m/z* 1351.7413 and 906.8186 corresponding to the bi- $[M+H+Na]^{2+}$ and tri-charged $[M+2H+K]^{3+}$ molecular ions of a 2679 Da PLTX (data not shown). Molecular ion fragmentation tests showed that collision-induced dissociation (CID) gave the best results using collision energies of 45 eV for bi- and tri-charged molecular ions and 100 eV for the mono-charged molecular ions. In the three *Palythoa* samples, fragmentation of the PLTX molecular ions produced a fragment ion at *m/z* 327 $[M+H]^{+}$ in the full MS spectra (supplementary informations, Fig. B), which corresponds to the characteristic PLTX A-moiety ($C_{16}H_{27}N_2O_5$) and results from the cleavage between carbon 8 and 9. For *P. heliodiscus* (Z07), fragmentation of the bishomo-PLTX bi- and tri-charged molecular ions produced a fragment ion at *m/z* 355 (supplementary informations, Fig. B) corresponding to the bishomo-PLTX A-moiety ($C_{18}H_{31}N_2O_5$) and also resulting from the cleavage between carbon 8 and 9. These results confirmed the presence of both PLTX and bishomo-PLTX in *P. heliodiscus* (Z07) tissues.

Distribution of PLTX and Symbiodiniaceae cells

Sagittal and cross-sections were analysed by MALDI-IMS to localize PLTX only in tissues of *Palythoa* sp. Z05 (representative of three polyps). Indeed, our access to the biological material was sometimes limited, in particular for *P.* aff. *clavata* (Z26 and Z27). Likewise, during handling, polyps closely related to *P. heliodiscus* (Z03, Z04, and Z07) decreased in size because of strong body contraction and secreted large amount of mucus that makes them poor candidates to carry out histological sectioning. Thus, we only selected Z05 specimen for MALDI-IMS because they were the biggest ones, with a solid body and producing less amount of mucus. It also exhibited the highest PLTX content allowing to expect a strong signal. PLTX was easily identified by MALDI-IMS and displayed a non-homogeneous distribution in polyp tissues (Fig. 5). The ectodermal tissues, e.g. the epidermis of the body wall and the pharynx, exhibited the highest concentrations (Fig. 5A, B). PLTX was also found in some tissues of endodermal origin but with concentrations usually lower than in the ectodermal ones (Fig. 5A–F). Among the endodermal tissues, the outer side of the endodermal fold close to the epidermis and the inner layer around the pharynx contained the highest PLTX concentrations (Fig. 5A, B). A very small amount of PLTX was detected in the gastrodermis of the enteron and septa (Fig. 5C–F). High concentrations of PLTX were also detected in the mucus-like secretion surrounding the polyps, especially well visible in the sagittal sections executed along the apical-basal axis of the body (data not shown). No PLTX was observed in the tentacles whatever the tissue considered (Fig. 5A, B). Sections were also analysed by epifluorescence microscopy to localize the endogenous autofluorescence due to chlorophyll and peridinin pigments of the Symbiodiniaceae cells (Fig. 5G–I). A strong signal was detected in the epidermis of both the body wall and the tentacles, the endodermal fold (outer layer of the gastrodermis below the epidermis) at the level of the mouth opening and the inner layer of the gastrodermis constituting the enteron wall. The gastrodermis constituting the septa walls located in the median part of the body also contained numerous Symbiodiniaceae cells (Fig. 5H), the number of which significantly decreased towards the apex (Fig. 5G) and the base (Fig. 5I).

Discussion

Zoantharia species identification

The unambiguous identification of a zoantharian species is a difficult task due to the lack of reliable diagnostic characters

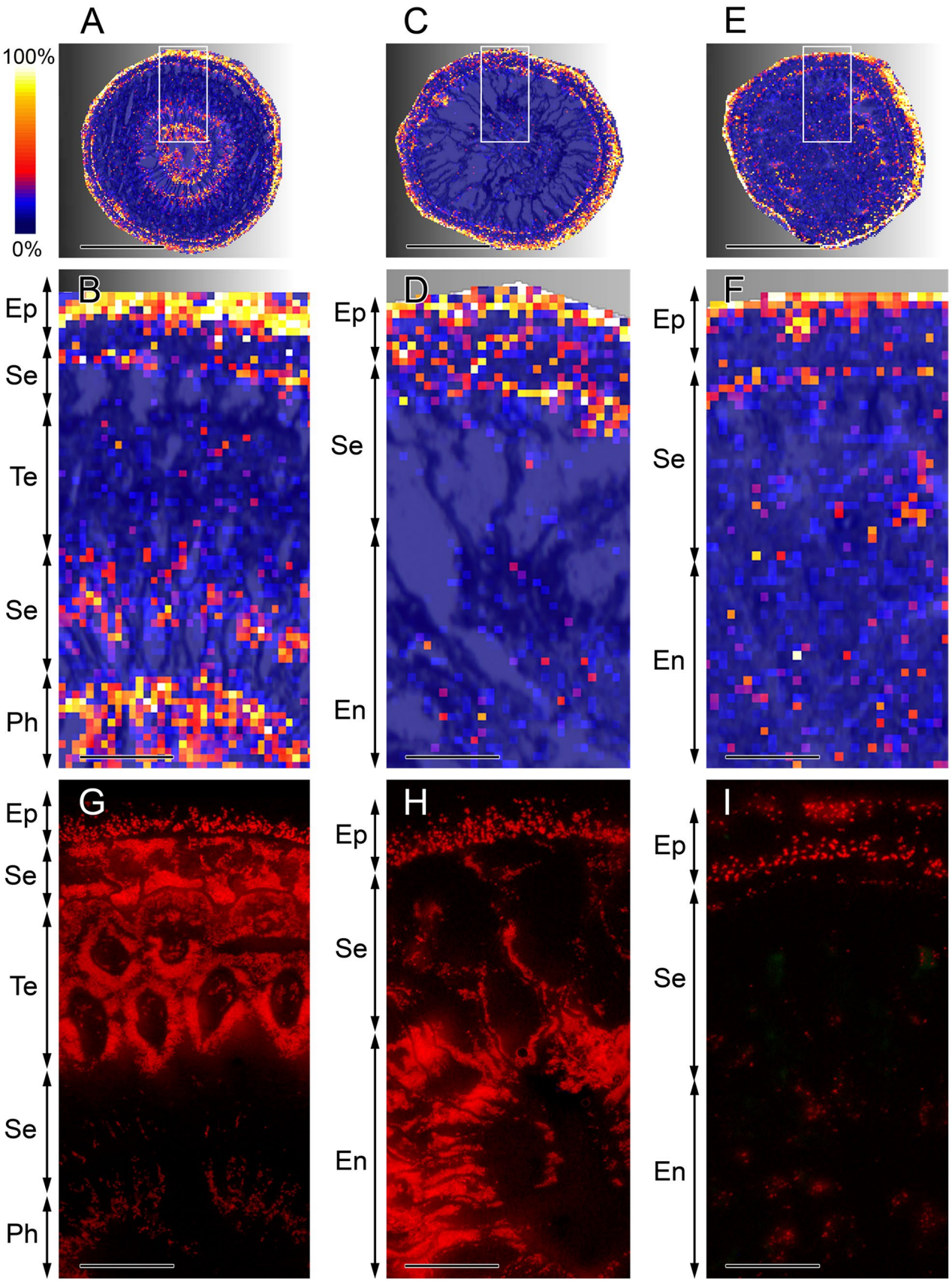
A
C
E
100%
0%
B
D
F
Ep
Se
Te
Se
Ph
Ep
Se
En
Ep
Se
En
G
H
I
Ep
Se
Te
Se
Ph
Ep
Se
En
Ep
Se
En

◂**Fig. 5** Cross-sections of *Palythoa* sp. Z05. Sections at the mouth and tentacles (**A**), actinopharynx (**C**), and basal peduncle (**E**) levels, demonstrating the location and relative concentrations of palytoxin (PLTX) by MALDI-imaging mass spectrometry. Areas delimited by white rectangles are enlarged (**B**, **D**, **F**) and compared with images of the same histological regions exhibiting endogenous autofluorescence due to photosynthetic pigments of Symbiodiniaceae cells (G-I). Abbreviations: En, enteron; Ep, epidermis; Ph, pharynx; Se, septa; Te, tentacles. Colour scale, the highest PLTX concentrations (100%) – no PLTX (0%). Scale bars = 3 mm (A, C, E), 0.5 mm (B, D, F, G-I)

and high levels of intraspecific morphological variation mainly marked in their oral disk colour pattern and the form of the colony (Burnett et al., 1997; Reimer et al., 2004, 2012). Six cases of intraspecific morphological plasticity were seen among the *Palythoa* and *Zoanthus* colonies used in this study: (1) *P.* aff. *clavata* Z26 and Z27; (2) *P. mutuki* Z06 and Z29; (3) *P. heliodiscus* Z03, Z04, and Z07; (4) *Z. kuroshio* Z14 and Z21; (5) *Z. sociatus/sansibaricus* Z15, Z17, Z23–Z25, and Z28; (6) *Z. gigantus/solanderi* Z08–Z13. In all cases, these zoantharians had either identical or very similar COI and ITS-rDNA sequences whereas colour phenotypes varied considerably (see supplementary informations, Fig. A). In addition to this, a previous phylogenetic study based on mitochondrial and nuclear sequences indicated that *Z. vietnamensis* and *Z. kuroshio* might be conspecific (Reimer et al., 2006a).

Both our COI and ITS-rDNA tree patterns confirmed the previous topology of *Zoanthus* and *Palythoa* species, which displayed complexes of sibling species pairs between the Caribbean and Indo-Pacific regions (Reimer et al., 2012). Indeed, in our results, the *Palythoa* species are clustered into three complexes: (1) *P. caribaeorum/tuberculosa*, (2) *P.* aff. *clavata*/sp. "sakurajimensis," and (3) *P. variabilis/heliodiscus*. *Zoanthus* species were also divided into three complexes: (1) *Z. pulchellus/kuroshio*, (2) *Z. sociatus/sansibaricus*, and (3) *Z. solanderi/gigantus*. These sibling species pairs result from the closure of the Isthmus of Panama 3 million years ago (Holcombe & Moore, 1977; O'Dea et al., 2016) and they consist of genetically identical or closely similar zoantharians that were previously named differently depending on their external morphology and location (Caribbean-Atlantic or Indo-Pacific regions) (Reimer et al., 2012). *P. grandis*, known for its endemism in the Caribbean Sea, is the only sample that does not fit into any of the complexes listed above and does not have any recorded sister species in the Indo-Pacific basin. These findings are congruent with those of Reimer et al. (2012). Finally, our molecular analyses showed that *Palythoa* sp. Z05 is a putatively undescribed Indo-Pacific species. Its closest relative is *P.* aff. *clavata* found in Florida waters (Reimer et al., 2012). The morphology of *Palythoa* sp. Z05 does not match conclusively with any Indo-Pacific described species but displays striking similarities with a specimen from the Cape Verde Islands named *Palythoa* sp. 265 (Reimer et al., 2010) which is also genetically very close to *P.* aff. *clavata* (Reimer et al., 2012). Later, Reimer et al. (2014) identified new specimens from Ascension Island belonging to the *clavata* complex. Both COI and ITS-rDNA markers have shown that the undescribed Indo-Pacific species *P.* sp. "sakurajimensis" is close to *Palythoa* sp. Z05. However, this last result is not congruent with morphological data, emphasizing once more that, in zoantharians, genetic similarities do not necessarily reflect morphological ones. In general, species boundaries are primarily based on morphology and it is usually assumed that morphological variations reflect reproductive isolation along with genetic differentiation. However, genetic studies and fertilization trials producing viable larvae suggest that morphological and genetic distinctions do not always correlate in corals (for a review see Miller & Benzie, 1997). Hybridization on coral reefs is common and widespread (for a review see Richards & Hobbs, 2015). So far, even if it is reasonable to consider *Palythoa* sp. Z05 as an undescribed species based on its morphology and location of collection, it is not possible to assess to which extent hybridization with colonies of *P.* sp. "sakurajimensis" occurs naturally on the reef.

Symbiodiniaceae diversity

According to previous studies, different Zoantharia species may have different patterns of association with Symbiodiniaceae (Reimer et al., 2013). In *Zoanthus* samples, our results highlighted a correlation between the geographical origin of the colony and the Symbiodiniaceae taxon. Indo-Pacific species predominantly hosted *Cladocopium* (*Z. kuroshio*, 3/3; *Z. sansibaricus*, 4/5) and *Durusdinium* (*Z. gigantus*, 1/1) whereas most species from the Caribbean-Atlantic basin hosted *Symbiodinium* (*Z. solanderi*, 5/5; *Z.* aff. *pulchellus*, 2/3; *Z. sociatus*, 1/1). These findings are consistent with previous studies that identified Symbiodiniaceae belonging to the genus *Cladocopium* in Indo-Pacific *Zoanthus* species sampled in Japanese coastal waters (Reimer & Todd, 2009; Reimer et al., 2013) while the genus *Symbiodinium* was predominant in colonies collected in coastal waters off Cape Verde and Brazil (Reimer et al., 2010; Fontenele Rabelo et al., 2014; López et al., 2019). However, all *Zoanthus* specimens, including *Z. pulchellus*, *Z.* aff. *pulchellus*, and *Z. solanderi*, collected in the Canary Islands hosted *Cladocopium* (López et al., 2019). *Cladocopium* is considered an Indo-Pacific generalist, known from multiple hosts and environment (Reimer et al., 2006c). According to Finney et al. (2010), who analysed the Symbiodiniaceae diversity of 45 genera of Cnidaria, symbiont specificity in the Caribbean is higher than that observed in the Indo-Pacific where *Cladocopium* dominates in many coral communities. This

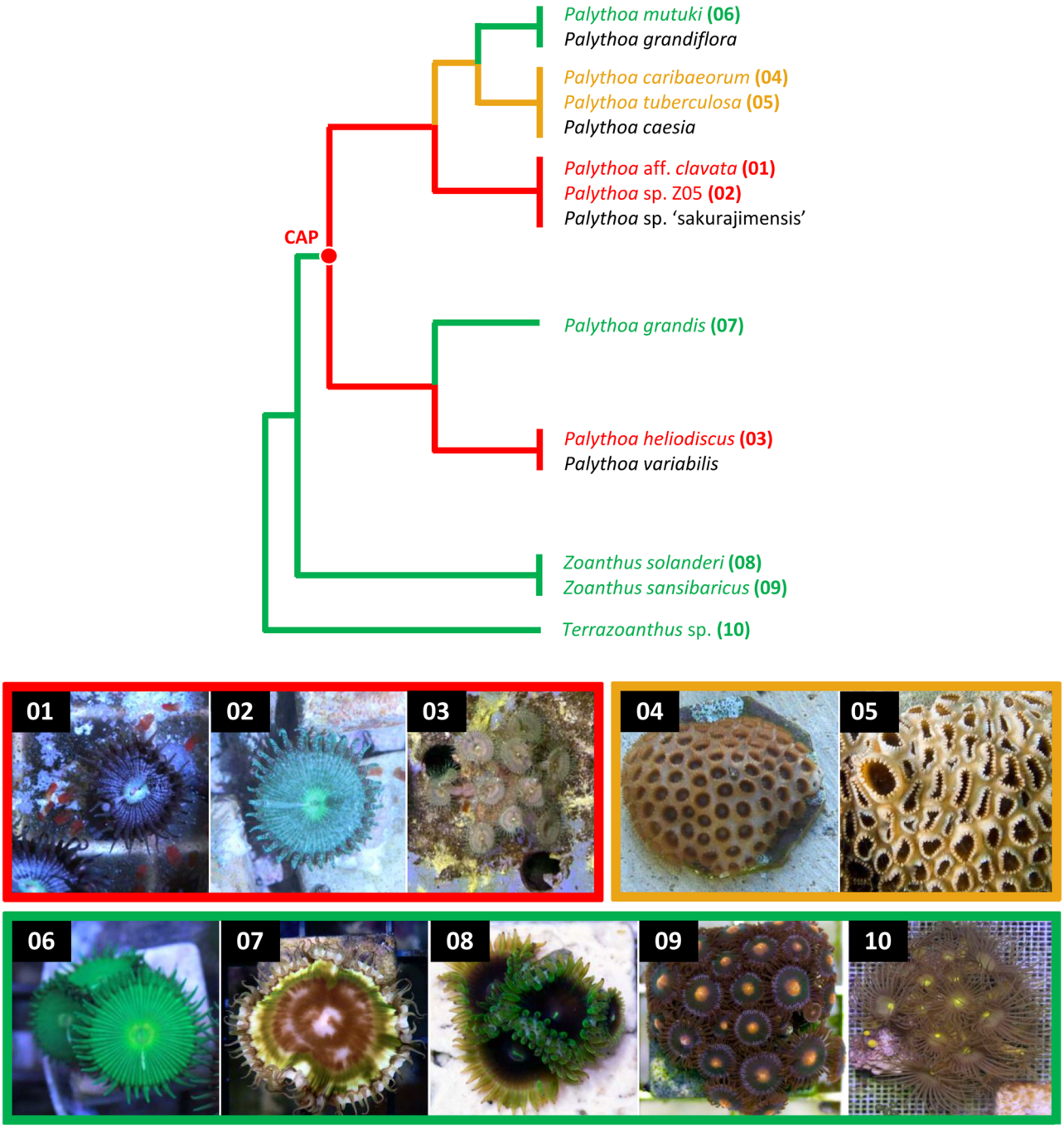

Fig. 6 Palytoxin (PLTX) contents in the genera *Palythoa*, *Terrazoanthus*, and *Zoanthus* determined in the present and previous studies. Red: high PLTX concentration (> 300 µg/g wet). Orange: weak PLTX concentration. Green: no PLTX detected. Black: not determined. CAP: common ancestor of all *Palythoa* species. *Palythoa tuberculosa* (Esper, 1805) has not been used in the present study but Hirata et al. (1979) measured low concentration of PLTX (10 µg/g wet *Palythoa*) in this species. Similarly, Béress et al. (1983) were able to find 30 µg/g in wet *Palythoa caribaeorum* (Duchassaing and Michelotti, 1860). In contrast to an earlier report (Gleibs et al., 1995) and according to our results and the study of Arakate et al. (2016), PLTX or PLTX-like compounds were only detected in *Palythoa* colonies but not in other zoantharians such as *Zoanthus* or *Terrazoanthus*. Scale bars = 1 cm

could be influenced by geographical isolation and habitat depth correlated with changes in ambient irradiance. Indeed, it has been shown that stress tolerant *Symbiodinium* and *Durusdinium* perform well at high irradiance and high temperature respectively and can increase bleaching resistance of the host (LaJeunesse et al., 2009; Silverstein et al.,

2015; Wang et al., 2012). In our study, the predominance of *Symbiodinium* spp. in *Z. solanderi*, *Z. sociatus*, and *Z.* aff. *pulchellus* from the Caribbean might suggest an adaptation to the environment in relation to abiotic stress tolerance. A similar strategy has been described in several Indo-Pacific zoantharian species collected in the Persian Gulf (*Symbiodinium* spp. predominant) which was also interpreted as an adaptation to isolated regions characterized by an extreme physical environment (Koupaei et al., 2016).

All *Palythoa* species analysed in this study were associated with Symbiodiniaceae belonging to the generalist genus *Cladocopium*. This same genus has been observed in all samples of *P. tuberculosa* and *P. mutuki* harvested in Japanese waters (Mizuyama et al., 2020; Reimer et al., 2006c) as well as in colonies of the Penghu Islands of Taiwan (Reimer et al., 2013). Similarly, all specimens of *P.* aff. *clavata*, *P. grandiflora*, and *P. caribaeorum* examined from the Canary and Cape Verde Archipelagos hosted *Cladocopium*, regardless of location or depth (López et al., 2019). However, previous studies in *Palythoa* species revealed that their Symbiodiniaceae diversity is somewhat flexible being associated either with *Cladocopium* or *Durusdinium*, notably for *Palythoa caesia* Dana, 1846 from the Indian Ocean (Burnett, 2002), *P. tuberculosa* and *P. mutuki* in Singapore waters (Reimer & Todd, 2009) and in the northern Persian Gulf (Koupaei et al., 2016) and *P. tuberculosa* in the Red sea (Reimer et al., 2017a) and the South China Sea off the Vietnam coasts (Sikorskaya et al., 2021). Our results, at least for the genus *Zoanthus*, support the idea that Symbiodiniaceae diversity is influenced by regional distribution and ecological specialisation, as previously suggested (Mizuyama et al., 2020; Reimer et al., 2017b; Wee et al., 2020).

Interspecific and intraspecific toxicity variability in Zoantharia

One of the goals of this study was to use the evolutionary relationships revealed by molecular phylogenetic analyses, as well as the comparative analysis of PLTX contents, to predict zoantharian toxicity in a phylogenetic context and investigate the relation between toxicity and Symbiodiniaceae strains. To date, only one study of the relation between toxicity and phylogeny in Zoantharia has been conducted, with a reduced-scale taxonomic sampling (Deeds et al., 2011). To assess the potential exposure of PLTX to marine aquarium hobbyists, specimens were identified through genetic analysis of 16S and COI markers. They investigated 16 specimens and tested the toxicity for the first time. They found four toxic specimens closely related to *P. heliodiscus* containing PLTX and PLTX-like compounds (range 0.5–3.5 mg/g wet zoantharian). Hamade et al. (2015) reported 7.3 mg and 6.2 mg/g wet zoantharian of PLTX in two specimens consistent with *P. heliodiscus*. These authors did not identified another PLTX analogue in these highly toxic specimens.

In the present study, none of the *Zoanthus* and *Terrazoanthus* tested contained PLTX or PLTX-like compounds but we observed toxicity variations in *Palythoa*. Specimens belonging to the *heliodiscus* complex were highly toxic which is consistent with the earlier findings of Deeds et al. (2011). Our results also demonstrated, for the first time, the presence of PLTX molecules in *P.* aff. *clavata* (Z26, Z27), an undescribed species from the Atlantic Ocean. *Palythoa* sp. Z05, another undescribed species from Indo-Pacific of the *clavata* complex, contains one of the highest amount of PLTX ever found in a zoantharian (2.22 ± 0.410 mg/g wet zoantharian). The mean recorded value of 0.22% (w/w) PLTX is high compared to the values found in the literature (see Table 1) and is eight times more than the first value of 0.027% (w/w) recorded by Moore and Scheuer (1971) from *Palythoa toxica* (Walsh & Bowers, 1971). Fraga et al. (2017) demonstrated the presence of PLTX, 42-OH-PLTX, and six minor PLTX-like molecules in *Palythoa canariensis* Haddon and Duerden, 1896, a species which has been considered a junior synonym to *P.* aff. *clavata* based on molecular data (López et al., 2019). The PLTX content in *P. canariensis* was estimated at 0.27 mg/g of lyophilized zoantharian using UPLC-IT-TOF–MS. In the sample of *P. heliodiscus* (Z07), we identified a mixture of bishomo-PLTX and PLTX. Although the concentration was high and corresponded to 0.16% (w/w), it was lower than the deoxy-PLTX concentration of 0.35% (w/w) measured in the same species by Deeds et al. (2011) who also found a maximum of 1.164 mg/g wet zoantharian of PLTX corresponding to 0.12% (w/w). This result is very close to the concentrations of PLTX measured in both the purple (Z27, 0.13%) and the green (Z26, 0.11%) morphotypes of *P.* aff. *clavata*.

The PLTX molecule identified in *Palythoa* sp. Z05, *P.* aff. *clavata* (Z26, Z27) and *P. heliodiscus* (Z07) has a molecular weight of 2679 Da corresponding to the PLTX previously found in *P. tuberculosa*, *P. toxica*, *P. caribaeorum* and *P. heliodiscus* (Béress et al., 1983; Deeds et al., 2011; Kimura & Hashimoto, 1973; Moore & Scheuer, 1971). The bishomo-PLTX isolated from *P. heliodiscus* (Z07) has a molecular weight of 2706 Da and is identical to the toxin identified in *P. tuberculosa* (Uemura et al., 1985). Finally, no PLTX or PLTX-like compounds were observed in *P. mutuki*, *P. caribaeorum* and *P. grandis* analysed in this study. Taken together, these results show a certain variability in both inter- and intraspecific toxicity in *Palythoa*. According to the most parsimonious scenario, phylogenetic patterns associated with comparative toxicity analysis suggest that the ability to produce and store a large amount of PLTX is likely a plesiomorphic character inherited from the last common ancestor of all *Palythoa* species that would have been lost independently in several lineages (Fig. 6).

All toxic species investigated in this study were associated with Symbiodiniaceae belonging to the generalist genus *Cladocopium* which is the most species-rich, ecologically abundant, and broadly distributed genus within the Symbiodiniaceae (LaJeunesse et al., 2018; Thornhill et al., 2014). While ITS2 of the rRNA gene remains the most popular marker used to infer the Symbiodiniaceae systematics (Shi et al., 2021), the species genetic delineation within *Cladocopium* is generally very difficult due to a very low interspecies variability in these sequences (Mizuyama et al., 2020; Reimer et al., 2017b; Thornhill et al., 2014). Considering ecological, geographic, reproductive, and genetic patterns, *Cladocopium* may consist of hundreds of species (Thornhill et al., 2014). If so, there are likely distinct *Cladocopium* species present within toxic species of *Palythoa*, the identification of which may only be demonstrated with higher phylogenetic resolution markers (LaJeunesse & Thornhill, 2011; Noda et al., 2017; Reimer et al., 2017b). To further describe the relationships between the *Cladocopium* strains and toxicity variability of their *Palythoa* hosts, it will be necessary to carry out studies based on alternative markers such as, for example, the plastid mini-circle non-coding region (Mizuyama et al., 2020; Moore et al., 2003; Reimer et al., 2017b; Takishita et al., 2003). Meta-barcoding using NGS-based analyses should be also carried out for a more detailed picture of intra- and interspecific ITS diversity (see Hume et al., 2019).

Biosynthesis and storage of PLTX in *Palythoa* species

Since its first isolation in 1971 by Moore and Scheuer, the origin of PLTX in *Palythoa* spp. is still a matter of debate. So far, the toxin synthetic pathway and the putative symbiotic organism(s) involved are entirely unknown. The main current hypothesis claims that the endosymbiotic Symbiodiniaceae is responsible for the presence of PLTX in *Palythoa* species (Drainville-Higgins, 2004; Nakamura et al., 1993; Onodera et al., 2004). However, the lack of correlation between chlorophyll a and PLTX contents contradicted its role in toxin synthesis (Gleibs et al., 1995). The implication of other potential producers, such as symbiotic prokaryotes, which can synthesize PLTX-like secondary metabolites may also be considered (Nakamura et al., 1993; Frolova et al., 2000; Seemann et al., 2009; Kerbrat et al., 2011). Interestingly, a PLTX-like haemolytic activity was identified in bacteria isolated from *P. caribaeorum* (Seemann et al., 2009) showing that some symbiotic bacteria alone can produce at least one PLTX type. In this study, MALDI-IMS analysis carried out for the first time on histological cross-sections through a *Palythoa* specimen showed that high levels of PLTX were not exclusively colocalised with Symbiodiniaceae cells, notably in the epidermis of the body wall and the pharynx. It should be noted that we also carried out cultures of Symbiodiniaceae cells isolated from *Palythoa* sp. Z05 and *P. heliodiscus*, but we could not show that these isolated cells constituted the exclusive PLTX producers (data not shown). All this evidence certainly suggests that the sole implication of *Cladocopium* is unlikely and supports the involvement of others symbiotic microorganisms as well as the cnidarian host to produce and store PLTX. This could explain the toxicity differences observed between genetically close species of *Palythoa* hosting genetically close Symbiodiniaceae of the genus *Cladocopium*, as illustrated by our molecular results. Accordingly, this could mean that the holobiont itself holds a decisive role in providing a favourable environment where crucial organisms are united for the synthesis and storage of PLTX.

In conclusion, this study partially answers the long-standing question on the origin of PLTX in zoantharians. Molecular phylogenies combined with chemical analyses showed that the ability to produce and store high levels of PLTX and/or its analogues in some *Palythoa* species could be inherited from their last common ancestor and subsequently lost in several lineages. All toxic and non-toxic *Palythoa* species hosted *Cladocopium* Symbiodiniaceae (formerly the generalist Symbiodinium clade C). Analysis of PLTX distribution in *Palythoa* tissues showed that high levels of toxin do not colocalised with *Cladocopium* cells. This suggests that the sole implication of Symbiodiniaceae cells is unlikely and support the involvement of the holobiont (host plus its microbiote) in the synthesis and storage of PLTX. So far, transcriptomic analyses on the coral holobiont have essentially focused on environmental factors implicated in bleaching events including temperatures, acidification, nutrient stress, and disease (Gierz et al., 2017). To identify the microorganism(s) involved in the PLTX synthesis in *Palythoa*, future integrative approaches incorporating transcriptomic and metabolomics should focus on the ability to produce PLTX in various types of holobionts and under different environmental conditions.

Supplementary Information The online version contains supplementary material available at https://doi.org/10.1007/s13127-022-00550-2.

Acknowledgements We are deeply grateful to James Reimer for helpful discussions on the systematics and phylogeny of Zoantharia during this study. The authors also wish to thank Daniel Papillon who provided English corrections. Sampling of zoantharians by diving in the Caribbean was made possible by a commercial MLD collection license from the US Government (State of Florida SPL #932658 with MLD endorsement #1117).

Author contribution LS and YP carried out the molecular experiments and phylogenetic analyses. LS and JL did the PLTX purification, HPLC, and mass spectrometry experiments. LS, CN, and JL did the MALDI-IMS analyses. CF collected specimens of *Zoanthus* and *Palythoa* species in Florida and maintained the clonal populations of *Palythoa* aff. *clavata* and *P. heliodiscus*. JL, YP, and LS drafted the

manuscript. JL and YP conceived and supervised the study. All authors read, amended, and approved the final manuscript.

Data availability All sequences generated in this study have been deposited and accepted in GenBank (MW077616 to MW077644, MW219226 to MW219250, MW717422 to MW717450). The datasets generated during and/or analysed during the current study are available from the corresponding author on reasonable request.

Declarations

Competing interests The authors declare no competing interests.

References

Aguilar, C., & Reimer, J. D. (2010). Molecular phylogenetic hypotheses of *Zoanthus* species (Anthozoa: Hexacorallia) using RNA secondary structure of the internal transcribed spacer 2 (ITS2). *Marine Biodiversity, 40*, 195–204. https://doi.org/10.1007/s12526-010-0043-2

Aratake, S., Taira, Y., Fujii, T., Roy, M. C., Reimer, J. D., Yamazaki, T., & Jenke-Kodama, H. (2016). Distribution of palytoxin in coral reef organisms living in close proximity to an aggregation of *Palythoa tuberculosa*. *Toxicon, 111*, 86–90. https://doi.org/10.1016/j.toxicon.2015.12.004

Barbany, M., Rossell, M., & Salvador, A. (2019). Toxicidad corneal por exposición a palitoxina [Toxic corneal reaction due to exposure to palytoxin]. *Archivos de la Sociedad Española de Oftalmología, 94*(4), 184–187. https://doi.org/10.1016/j.oftal.2018.10.011

Béress, L., Zwick, J., Kolkenbrock, H. J., Kaul, P. N., & Wassermann, O. (1983). A method for the isolation of the caribbean palytoxin (C-PTX) from the coelenterate (zoanthid) *Palythoa caribaeorum*. *Toxicon, 21*(2), 285–290. https://doi.org/10.1016/0041-0101(83)90013-2

Burnett, W. J., Benzie, J. A. H., Beardmore, J. A., & Ryland, J. S. (1997). Zoanthids (Anthozoa, Hexacorallia) from the Great Barrier Reef and Torres Strait, Australia: Systematics, evolution and a key to species. *Coral Reefs, 16*, 55–68. https://doi.org/10.1007/s003380050060

Burnett, W. J. (2002). Longitudinal variation in algal symbionts (zooxanthellae) from the Indian Ocean zoanthid *Palythoa caesia*. *Marine Ecology Progress Series, 234*, 105–109. https://doi.org/10.3354/meps234105

Chang, E., Deeds, J., & Spaeth, K. (2020). A case of long-term neurological and respiratory sequelae of inhalational exposure to palytoxin. *Toxicon, 186*, 1–3. https://doi.org/10.1016/j.toxicon.2020.07.018

Ciminiello, P., Dell'Aversano, C., Fattorusso, E., Forino, M., Tartaglione, L., Grillo, C., & Melchiorre, N. (2008). Putative palytoxin and its new analogue, ovatoxin-a, in *Ostreopsis ovata* collected along the Ligurian coasts during the 2006 toxic outbreak. *Journal of the American Society for Mass Spectrometry, 19*(1), 111–120. https://doi.org/10.1016/j.jasms.2007.11.001

Ciminiello, P., Dell'aversano, C., Dello Iacovo, E., Fattorusso, E., Forino, M., Grauso, L., Tartaglione, L., Florio, C., Lorenzon, P., De Bortoli, M., Tubaro, A., Poli, M., & Bignami, G. (2009). Stereostructure and biological activity of 42-hydroxy-palytoxin: A new palytoxin analogue from Hawaiian *Palythoa* subspecies. *Chemical Research in Toxicology, 22*(11), 1851–1859. https://doi.org/10.1021/tx900259v

Costa, D. L., Gomes, P. B., Santos, A. M., Valença, N. S., Vieira, N. A., & Pérez, C. D. (2011). Morphological plasticity in the reef zoanthid *Palythoa caribaeorum* as an adaptive strategy. *Annales Zoologici Fennici, 48*(6), 349–358.

Deeds, J. R., Handy, S. M., White, K. D., & Reimer, J. D. (2011). Palytoxin found in *Palythoa* sp. zoanthids (Anthozoa, Hexacorallia) sold in the home aquarium trade. *PloS One 6*(4), e18235. https://doi.org/10.1371/journal.pone.0018235

Del Favero, G., Sosa, S., Pelin, M., D'Orlando, E., Florio, C., Lorenzon, P., Poli, M., & Tubaro, A. (2012). Sanitary problems related to the presence of Ostreopsis spp. in the Mediterranean Sea: A multidisciplinary scientific approach. *Annali dell'Istituto Superiore di Sanità, 48*(4), 407–414. https://doi.org/10.4415/ANN_12_04_08

Drainville-Higgins, K. E. (2004). Isolation of marine metabolites from *Symbiodinium* species of dinoflagellates. Doctoral dissertation, The University of Rhode Island.

Edgar, R. C. (2004). MUSCLE: Multiple sequence alignment with high accuracy and high throughput. *Nucleic Acids Research, 32*(5), 1792–1797. https://doi.org/10.1093/nar/gkh340

Farooq, A. V., Gibbons, A. G., Council, M. D., Harocopos, G. J., Holland, S., Judelson, J., Shoss, B. L., Schmidt, E. J., Md Noh, U. K., D'Angelo, A., Chundury, R. V., Judelson, R., Perez, V. L., & Huang, A. J. W. (2017). Corneal toxicity associated with aquarium coral palytoxin. *American Journal of Ophthalmology, 174*, 119–125. https://doi.org/10.1016/j.ajo.2016.10.007

Finney, J. C., Pettay, D. T., Sampayo, E. M., Warner, M. E., Oxenford, H. A., & LaJeunesse, T. C. (2010). The relative significance of host-habitat, depth, and geography on the ecology, endemism, and speciation of coral endosymbionts in the genus *Symbiodinium*. *Microbial Ecology, 60*(1), 250–263. https://doi.org/10.1007/s00248-010-9681-y

Fontenele Rabelo, E., Leal Rocha, L., Barguil Colares, G., & Araujo Bomfim, T. (2014). *Symbiodinium* diversity associated with zoanthids (Cnidaria: Hexacorallia) in Northeastern Brazil. *Symbiosis, 64*, 105–113. https://doi.org/10.1007/s13199-014-0308-9

Fraga, M., Vilariño, N., Louzao, M. C., Molina, L., López, Y., Poli, M., & Botana, L. M. (2017). First identification of palytoxin-like molecules in the Atlantic coral species *Palythoa canariensis*. *Analytical Chemistry, 89*(14), 7438–7446. https://doi.org/10.1021/acs.analchem.7b01003

Frolova, G. M., Kuznetsova, T. A., Mikhailov, V. V., & Elyakov, G. B. (2000). An enzyme linked immunosorbent assay for detecting palytoxin-producing bacteria. *Russian Journal of Bioorganic Chemistry, 26*(4), 285–289. https://doi.org/10.1007/BF02759168

Gaudchau, A., Pfeiffer, N., & Gericke, A. (2019). Verätzung durch Krustenanemone [Chemical burns caused by crust anemone]. *Der Ophthalmologe, 116*, 376–379. https://doi.org/10.1007/s00347-018-0742-9

Gierz, S. L., Forêt, S., & Leggat, W. (2017). Transcriptomic analysis of thermally stressed *Symbiodinium* reveals differential expression of stress and metabolism genes. *Frontiers in Plant Science, 8*, 271. https://doi.org/10.3389/fpls.2017.00271

Gleibs, S., Mebs, D., & Werding, B. (1995). Studies on the origin and distribution of palytoxin in a Caribbean coral reef. *Toxicon, 33*(11), 1531–1537. https://doi.org/10.1016/0041-0101(95)00079-2

Hall, T. A. (1999). BioEdit: A user-friendly biological sequence alignment editor and analysis program for Windows 95/98/NT. *Nucleic Acids Symposium Series, 41*, 95–98.

Hall, C., Levy, D., & Sattler, S. (2015). A case of palytoxin poisoning in a home aquarium enthusiast and his family. *Case Reports in Emergency Medicine, 2015*, 1–3. https://doi.org/10.1155/2015/621815

Hamade, A. K., Deglin, S. E., McLaughlin, J. B., Deeds, J. R., Handy, S. M., & Knolhoff, A. M. (2015). Suspected palytoxin inhalation exposures associated with zoanthid corals in aquarium shops and

homes—Alaska, 2012–2014. *MMWR. Morbidity and Mortality Weekly Report, 64*(31), 852.
Hasegawa, M., Kishino, H., & Yano, T. (1985). Dating of the human-ape splitting by a molecular clock of mitochondrial DNA. *Journal of Molecular Evolution, 22*, 160–174. https://doi.org/10.1007/BF02101694
Hirata, Y., Uemura, D., Ueda, K., & Takano, S. (1979). Several compounds from *Palythoa tuberculosa* (Coelenterata). *Pure and Applied Chemistry, 51*(9), 1875–1883. https://doi.org/10.1351/pac197951091875
Holcombe, T. L., & Moore, W. S. (1977). Paleocurrents in the eastern Caribbean: Geologic evidence and implications. *Marine Geology, 23*(1–2), 35–56. https://doi.org/10.1016/0025-3227(77)90080-9
Hume, B. C. C., Smith, E. G., Ziegler, M., Warrington, H. J. M., Burt, J. A., LaJeunesse, T. C., Wiedenmann, J., & Voolstra, C. R. (2019). SymPortal: A novel analytical framework and platform for coral algal symbiont next-generation sequencing ITS2 profiling. *Molecular Ecology Resources, 19*(4), 1063–1080.
Jalink, M. B., & van Luijk, C. M. (2019). Wegsmeltende hoornvliezen na de verhuizing van een zeeaquarium [Corneal melting after moving a tropical aquarium]. *Nederlands Tijdschrift Voor Geneeskunde, 163*.
Kamezaki, M., Higa, M., Hirose, M., Suda, S., & Reimer, J. D. (2013). Different zooxanthellae types in populations of the zoanthid *Zoanthus sansibaricus* along depth gradients in Okinawa, Japan. *Marine Biodiversity, 43*, 61–70. https://doi.org/10.1007/s12526-012-0119-2
Kelmanson, I. V., & Matz, M. V. (2003). Molecular basis and evolutionary origins of color diversity in great star coral *Montastraea cavernosa* (Scleractinia: Faviida). *Molecular Biology and Evolution, 20*(7), 1125–1133. https://doi.org/10.1093/molbev/msg130
Kerbrat, A. S., Amzil, Z., Pawlowiez, R., Golubic, S., Sibat, M., Darius, H. T., Chinain, M., & Laurent, D. (2011). First evidence of palytoxin and 42-hydroxy-palytoxin in the marine cyanobacterium *Trichodesmium*. *Marine Drugs, 9*(4), 543–560. https://doi.org/10.3390/md9040543
Kimura, M. (1980). A simple method for estimating evolutionary rates of base substitutions through comparative studies of nucleotide sequences. *Journal of Molecular Evolution, 16*, 111–120. https://doi.org/10.1007/BF01731581
Kimura, S., & Hashimoto, Y. (1973). Purification of the toxin in a zoanthid *Palythoa tuberculosa*. *Publications of the Seto Marine Biological Laboratory, 20*, 713–718.
Koupaei, A. N., Dehghani, H., Mostafavi, P. G., & Mashini, A. G. (2016). Phylogeny of *Symbiodinium* populations in zoantharians of the northern Persian Gulf. *Marine Pollution Bulletin, 105*(2), 553–557. https://doi.org/10.1016/j.marpolbul.2016.02.058
LaJeunesse, T. C., Smith, R. T., Finney, J., & Oxenford, H. (2009). Outbreak and persistence of opportunistic symbiotic dinoflagellates during the 2005 Caribbean mass coral 'bleaching' event. *Proceedings of the Royal Society B: Biological Sciences, 276*(1676), 4139–4148. https://doi.org/10.1098/rspb.2009.1405
LaJeunesse, T. C., & Thornhill, D. J. (2011). Improved resolution of reef-coral endosymbiont (*Symbiodinium*) species diversity, ecology, and evolution through psbA non-coding region genotyping. *PLoS One, 6*(12), e29013. https://doi.org/10.1371/journal.pone.0029013
LaJeunesse, T. C., Parkinson, J. E., Gabrielson, P. W., Jeong, H. J., Reimer, J. D., Voolstra, C. R., & Santos, S. R. (2018). Systematic revision of Symbiodiniaceae highlights the antiquity and diversity of coral endosymbionts. *Current Biology, 28*(16), 2570–2580. https://doi.org/10.1016/j.cub.2018.07.008
Ledreux, A., Krys, S., & Bernard, C. (2009). Suitability of the Neuro-2a cell line for the detection of palytoxin and analogues (neurotoxic phycotoxins). *Toxicon, 53*(2), 300–308. https://doi.org/10.1016/j.toxicon.2008.12.005
Lenoir, S., Ten-Hage, L., Turquet, J., Quod, J. -P., Bernard, C., & Hennion, M. -C. (2004). First evidence of palytoxin analogues from an *Ostreopsis mascarenensis* (Dinophyceae) benthic bloom in southwestern Indian Ocean. *Journal of Phycology, 40*(6), 1042–1051. https://doi.org/10.1111/j.1529-8817.2004.04016.x
López, C., Reimer, J. D., Brito, A., Simón, D., Clemente, S., & Hernández, M. (2019). Diversity of zoantharian species and their symbionts from the Macaronesian and Cape Verde ecoregions demonstrates their widespread distribution in the Atlantic Ocean. *Coral Reefs, 38*(2), 269–283.
Low, M. E., Sinniger, F., & Reimer, J. D. (2016). The order Zoantharia Rafinesque, 1815 (Cnidaria, Anthozoa: Hexacorallia): supraspecific classification and nomenclature. *ZooKeys, 641*, 1–80. https://doi.org/10.3897/zookeys.641.10346
Miller, K. J., & Benzie, J. A. H. (1997). No clear genetic distinction between morphological species within the coral genus *Platygyra*. *Bulletin of Marine Science, 61*(3), 907–917.
Mizuyama, M., Iguchi, A., Iijima, M., Gibu, K., & Reimer, J. D. (2020). Comparison of Symbiodiniaceae diversities in different members of a *Palythoa* species complex (Cnidaria: Anthozoa: Zoantharia)–Implications for ecological adaptations to different microhabitats. *PeerJ, 8*, e8449. https://doi.org/10.7717/peerj.8449
Moore, R. E., & Scheuer, P. J. (1971). Palytoxin a new marine toxin from a Coelenterate. *Nature, 172*(3982), 495–498. https://doi.org/10.1126/science.172.3982.495
Moore, R. B., Ferguson, K. M., Loh, W. K., Hoegh-Guldberg, O., & Carter, D. A. (2003). Highly organized structure in the non-coding region of the psbA minicircle from clade C *Symbiodinium*. *International Journal of Systematic and Evolutionary Microbiology, 53*(6), 1725–1734. https://doi.org/10.1099/ijs.0.02594-0
Moshirfar, M., Khalifa, Y. M., Espandar, L., & Mifflin, M. D. (2010). Aquarium coral keratoconjunctivitis. *Archives of Ophthalmology, 128*(10), 1360–1362. https://doi.org/10.1001/archophthalmol.2010.206
Moshirfar, M., Hastings, J., Ronquillo, Y., & Patel, B. C. (2021). Palytoxin keratitis. In: StatPearls [Internet]. Treasure Island (FL): StatPearls Publishing; 2021 Jan–. PMID: 31985993.
Nakamura, H., Asari, T., Ohizumi, Y., Kobayashi, J., Yamasu, T., & Murai, A. (1993). Isolation of zooxanthellatoxins, novel vasoconstrictive substances from the zooxanthella *Symbiodinium* sp. *Toxicon, 31*(4), 371–376. https://doi.org/10.1016/0041-0101(93)90172-F
Noda, H., Parkinson, J. E., Yang, S. Y., & Reimer, J. D. (2017). A preliminary survey of zoantharian endosymbionts shows high genetic variation over small geographic scales on Okinawa-jima Island, Japan. *Peerj, 5*(2), e3740. https://doi.org/10.7717/peerj.3740
Nordt, S. P., Wu, J., Zahller, S., Clark, R. F., & Cantrell, F. L. (2011). Palytoxin poisoning after dermal contact with zoanthid coral. *The Journal of Emergency Medicine, 40*(4), 397–399. https://doi.org/10.1016/j.jemermed.2009.05.004
O'Dea, A., Lessios, H. A., Coates, A. G., Eytan, R. I., Restrepo-Moreno, S. A., et al. (2016). Formation of the Isthmus of Panama. *Science Advances, 2*(8), e1600883. https://doi.org/10.1126/sciadv.1600883
Oku, N., Sata, N. U., Matsunaga, S., Uchida, H., & Fusetani, N. (2004). Identification of palytoxin as a principle which causes morphological changes in rat 3Y1 cells in the zoanthid *Palythoa* aff. *margaritae*. *Toxicon, 43(1)*, 21–25. https://doi.org/10.1016/j.toxicon.2003.10.012
Ong, C. W., Reimer, J. D., & Todd, P. A. (2013). Morphologically plastic responses to shading in the zoanthids *Zoanthus sansibaricus* and *Palythoa tuberculosa*. *Marine Biology, 160*, 1053–1064. https://doi.org/10.1007/s00227-012-2158-4
Onodera, K., Nakamura, H., Oba, Y., & Ojika, M. (2004). Zooxanthellamide B, a novel large polyhydroxy metabolite from a marine dinoflagellate of *Symbiodinium* sp. *Bioscience, Biotechnology,*

and Biochemistry, 68(4), 955–958. https://doi.org/10.1271/bbb.68.955

Posada, D., & Crandall, K. A. (1998). MODELTEST: Testing the model of DNA substitution. *Bioinformatics, 14*(9), 817–818. https://doi.org/10.1093/bioinformatics/14.9.817

Quinn, R. J., Kashiwagi, M., Moore, R. E., & Norton, T. R. (1974). Anticancer activity of zoanthids and the associated toxin, palytoxin, against Ehrlich ascites tumor and P-388 lymphocytic leukemia in mice. *Journal of Pharmaceutical Sciences, 63*(2), 257–260. https://doi.org/10.1002/jps.2600630217

Reimer, J. D., & Todd, P. (2009). Preliminary molecular examination of zooxanthellate zoanthid (Hexacorallia, Zoantharia) and associated zooxanthellae (*Symbiodinium* spp.) diversity in Singapore. *The Raffles Bulletin of Zoology, 22*, 103–120.

Reimer, J. D., Ono, S., Fujiwara, Y., Takishita, K., & Tsukahara, J. (2004). Reconsidering *Zoanthus* spp. diversity: Molecular evidence of conspecifity within four previously presumed species. *Zoological Science, 21(5)*, 517–525. https://doi.org/10.2108/zsj.21.517

Reimer, J. D., Ono, S., Iwama, A., Tsukahara, J., & Maruyama, T. (2006a). High levels of morphological variation despite close genetic relatedness between *Zoanthus* aff. *vietnamensis* and *Zoanthus kuroshio* (Anthozoa: Hexacorallia). *Zoological Science, 23(9)*, 755–761. https://doi.org/10.2108/zsj.23.755

Reimer, J. D., Ono, S., Takishita, K., Tsukahara, J., & Maruyama, T. (2006b). Molecular evidence suggesting species in the zoanthid genera *Palythoa* and *Protopalythoa* (Anthozoa: Hexacorallia) are congeneric. *Zoological Science, 23*(1), 87–94. https://doi.org/10.2108/zsj.23.87

Reimer, J. D., Takishita, K., & Maruyama, T. (2006c). Molecular identification of symbiotic dinoflagellates (*Symbiodinium* spp.) from *Palythoa* spp. (Anthozoa: Hexacorallia) in Japan. *Coral Reefs, 25*, 521–527. https://doi.org/10.1007/s00338-006-0151-4

Reimer, J. D., Takishita, K., Ono, S., Tsukahara, J., & Maruyama, T. (2007). Molecular evidence suggesting interspecific hybridization in *Zoanthus* spp. (Anthozoa: Hexacorallia). *Zoological Science, 24(4)*, 46–359. https://doi.org/10.2108/zsj.24.346

Reimer, J. D., Hirose, M., & Wirtz, P. (2010). Zoanthids of the Cape Verde Islands and their symbionts: Previously unexamined diversity in the Northeastern Atlantic. *Contributions to Zoology, 79*(4), 47–163. https://doi.org/10.1163/18759866-07904002

Reimer, J. D., Foord, C., & Irei, Y. (2012). Species diversity of shallow water zoanthids (Cnidaria: Anthozoa: Hexacorallia) in Florida. *Journal of Marine Biology, 2012*, 1–14. https://doi.org/10.1155/2012/856079

Reimer, J. D., Irei, Y., Fujii, T., & Yang, S. -Y. (2013). Molecular analyses of shallow-water zooxanthellate zoanthids (Cnidaria: Hexacorallia) from Taiwan and their *Symbiodinium* spp. *Zoological Studies, 52*, 38. https://doi.org/10.1186/1810-522X-52-38

Reimer, J. D., Lorion, J., Irei, Y., Hoeksema, B. W., & Wirtz, P. (2014). Ascension Island shallow-water Zoantharia(Hexacorallia: Cnidaria) and theirzooxanthellae (Symbiodinium*). Journal of the Marine Biological Association of the United Kingdom, 97*(4), 695–703.

Reimer, J. D., Herrera, M., Gatins, R., Roberts, M. B., Parkinson, J. E., & Berumen, M. L. (2017a). Latitudinal variation in the symbiotic dinoflagellate *Symbiodinium* of the common reef zoantharian *Palythoa tuberculosa* on the Saudi Arabian coast of the Red Sea. *Journal of Biogeography, 44*(3), 661–673. https://doi.org/10.1111/jbi.12795

Reimer, J. D., Montenegro, J., Santos, M. E. A., Low, M. E. Y., Herrera Sarrias, M., Gatins, R., Roberts, M. B., & Berumen, M. L. (2017b). Zooxanthellate zoantharians (Anthozoa: Hexacorallia: Zoantharia: Brachycnemina) in the northern Red Sea. *Marine Biodiversity*. https://doi.org/10.1007/s12526-017-0706-3

Richards, Z. T., & Hobbs, J. P. A. (2015). Hybridisation on coral reefs and the conservation of evolutionary novelty. *Current Zoology, 61*(1), 132–145. https://doi.org/10.1093/czoolo/61.1.132

Ronquist, F., & Huelsenbeck, J. P. (2003). MrBayes 3: Bayesian phylogenetic inference under mixed models. *Bioinformatics, 19*(12), 1572–1574. https://doi.org/10.1093/bioinformatics/btg180

Rossi, R., Castellano, V., Scalco, E., Serpe, L., Zingone, A., & Soprano, V. (2010). New palytoxin-like molecules in Mediterranean *Ostreopsis* cf. *ovata* (dinoflagellates) and in *Palythoa tuberculosa* detected by liquid chromatography-electrospray ionization time-of-flight mass spectrometry. *Toxicon, 56*(8), 1381–1387. https://doi.org/10.1016/j.toxicon.2010.08.003

Ruiz, Y., Fuchs, J., Beuschel, R., Tschopp, M., & Goldblum, D. (2015). Dangerous reef aquaristics: Palytoxin of a brown encrusting anemone causes toxic corneal reactions. *Toxicon, 106*, 42–45. https://doi.org/10.1016/j.toxicon.2015.09.001

Schulz, M., Łoś, A., Szabelak, A., & Strachecka, A. (2019). Inhalation poisoning with palytoxin from aquarium coral: Case description and safety advice. *Archives of Industrial Hygiene and Toxicology, 70*(1), 14–17. https://doi.org/10.2478/aiht-2019-70-3209

Seemann, P., Gernert, C., Schmitt, S., Mebs, D., & Hentschel, U. (2009). Detection of hemolytic bacteria from *Palythoa caribaeorum* (Cnidaria, Zoantharia) using a novel palytoxin-screening assay. *Antonie Van Leeuwenhoek, 96*(4), 405–411. https://doi.org/10.1007/s1048-009-9353-4

Shi, T., Niu, G., Kvitt, H., Zheng, X., Qin, Q., Sun, D., Ji, Z., & Tchernov, D. (2021). Untangling ITS2 genotypes of algal symbionts in zooxanthellate corals. *Molecular Ecology Resources, 21*(1), 137–152. https://doi.org/10.1111/1755-0998.13250

Sikorskaya, T. V., Efimova, K. V., & Imbs, A. B. (2021). Lipidomes of phylogenetically different symbiotic dinoflagellates of corals. *Phytochemistry, 181*, 112579. https://doi.org/10.1016/j.phytochem.2020.112579

Silverstein, R. N., Cunning, R., & Baker, A. C. (2015). Change in algal symbiont communities after bleaching, not prior heat exposure, increases heat tolerance of reef corals. *Global Change Biology, 21*(1), 236–249. https://doi.org/10.1111/gcb.12706

Sinniger, F., Reimer, J. D., & Pawlowski, J. (2008). Potential of DNA sequences to identify zoanthids (Cnidaria: Zoantharia). *Zoological Science, 25*(12), 1253–1260. https://doi.org/10.2108/zsj.25.1253

Snoeks, L., & Veenstra, J. (2012). Family with fever after cleaning a sea aquarium. *Nederlands Tijdschrift Voor Geneeskunde, 156*(12), A4200.

Takishita, K., Ishikura, M., Koike, K., & Maruyama, T. (2003). Comparison of phylogenies based on nuclear-encoded SSU rDNA and plastid-encoded psbA in the symbiotic dinoflagellate genus *Symbiodinium*. *Phycologia, 42*(3), 285–291. https://doi.org/10.2216/i0031-8884-42-3-285.1

Tamura, K., Stecher, G., Peterson, D., Filipski, A., & Kumar, S. (2013). MEGA6: Molecular Evolutionary Genetics Analysis version 6.0. *Molecular Biology and Evolution, 30*(12), 2725–2729. https://doi.org/10.1093/molbev/mst197

Tartaglione, L., Pelin, M., Morpurgo, M., Dell'Aversano, C., Montenegro, J., Sacco, G., Sosa, S., Reimer, J. D., Ciminiello, P., & Tubaro, A. (2016). An aquarium hobbyist poisoning: Identification of new palytoxins in *Palythoa* cf. *toxica* and complete detoxification of the aquarium water by activated carbon. *Toxicon, 121*, 41–50. https://doi.org/10.1016/j.toxicon.2016.08.012

Terajima, T., Uchida, H., Abe, N., & Yasumoto, T. (2018). Simple structural elucidation of ostreocin-B, a new palytoxin congener isolated from the marine dinoflagellate *Ostreopsis siamensis*, using complementary positive and negative ion liquid chromatography/quadrupole time-of-flight mass spectrometry. *Rapid Communication in Mass Spectrometry, 32*(12), 1001–1007. https://doi.org/10.1002/rcm.8130

Terajima, T., Uchida, H., Abe, N., & Yasumoto, T. (2019). Structure elucidation of ostreocin-A and ostreocin-E1, novel palytoxin analogs produced by the dinoflagellate *Ostreopsis siamensis*, using LC/Q-TOF MS. *Bioscience, Biotechnology, and Biochemistry, 83*(3), 381–390. https://doi.org/10.1080/09168451.2018.1550356

Thornhill, D. J., Lewis, A. M., Wham, D. C., & LaJeunesse, T. C. (2014). Host-specialist lineages dominate the adaptive radiation of reef coral endosymbionts. *Evolution, 68*(2), 352–367. https://doi.org/10.1111/evo.12270. Epub 2013 Oct 17. PMID: 24134732.

Uemura, T., Hirata, Y., Iwashita, T., & Naoki, H. (1985). Studies on palytoxins. *Tetrahedron, 41*(6), 1007–1017. https://doi.org/10.1016/S0040-4020(01)96468-3

Ukena, T., Satake, M., Usami, M., Oshima, Y., Naoki, H., Fujita, T., Kan, Y., & Yasumoto, T. (2001). Structure elucidation of ostreocin D, a palytoxin analog isolated from the dinoflagellate *Ostreopsis siamensis*. *Bioscience, Biotechnology, and Biochemistry, 65*(11), 2585–2588. https://doi.org/10.1271/bbb.65.2585

Valverde, I., Lago, J., Reboreda, A., Vieites, J. M., & Cabado, A. G. (2008). Characteristics of palytoxin induced cytotoxicity in neuroblastoma cells. *Toxicology in Vitro, 22*(6), 1432–1439. https://doi.org/10.1016/j.tiv.2008.04.012

Wang, J.-T., Chen, Y.-Y., Chen, C. A., & Meng, P.-J. (2012). Determination of the thermal tolerance of *Symbiodinium* using the activation energy for inhibiting photosystem II activity. *Zoological Studies, 51*(2), 137–142.

Wee, H. B., Berumen, M. L., Ravasi, T., & Reimer, J. D. (2020). Symbiodiniaceae diversity of *Palythoa tuberculosa* in the central and southern Red Sea influenced by environmental factors. *Coral Reefs, 39*(6), 1619–1633. https://doi.org/10.1007/s00338-020-01989-5

Wonneberger, W., Claesson, M., & Zetterberg, M. (2020). Corneal perforation due to palytoxin exposure of domestic zoanthid corals. *Acta Ophthalmologica*. https://doi.org/10.1111/aos.14594

Yasumoto, T., & Murata, M. (1990). Polyether toxins involved in seafood poisoning. In S. Hall & G. Strichartz (Eds.), *Marine Toxins* (pp. 120–132). American Chemical Society.